













The biological basis for using optical signals to track evergreen needleleaf photosynthesis

Zoe Amie Pierrat , Troy S. Magney , Rui Cheng , Andrew J. Maguire , Christopher Y.S. Wong , Magali F. Nehemy , Mukund Rao , Sara E. Nelson, Anneka F. Williams, Jeremy A. Hoyne Grosvenor, Kenneth R. Smith, Jaret S. Reblin , Jochen Stutz , Andrew D. Richardson , Barry A. Logan , and David R. Bowling 

Zoe Amie Pierrat (zpierrat@ucla.edu, zoe.a.pierrat@jpl.nasa.gov), and Jochen Stutz are affiliated with the Department of Atmospheric and Oceanic Sciences at the University of California Los Angeles, in Los Angeles, California, in the United States. Zoe Amie Pierrat and Andrew J. Maguire are affiliated with the Jet Propulsion Laboratory at the California Institute of Technology, in Pasadena, California, in the United States. Troy S. Magney, Christopher Y. S. Wong, and Mukund Rao are affiliated with the Department of Plant Sciences at the University of California Davis, in Davis, California, in the United States. Rui Cheng is affiliated with the Department of Civil and Environmental Engineering at the Massachusetts Institute of Technology, in Cambridge, Massachusetts, in the United States. Andrew J. Maguire is affiliated with Conservation Science Partners, Inc., in Truckee, California, in the United States. Magali F. Nehemy is affiliated with the Trent School of the Environment, at Trent University, in Peterborough, Ontario, in Canada. Mukund Rao is affiliated with the Centre de Recerca Ecològica i Aplicacions Forestals, in Bellaterra (Barcelona), in Spain. Mukund Rao is affiliated with the Lamont-Doherty Earth Observatory of Columbia University, in Palisades, New York, in the United States. Sara E. Nelson, Anneka F. Williams, Jeremy A. Hoyne Grosvenor, and Barry A. Logan are affiliated with the Department of Biology at Bowdoin College, in Brunswick, Maine, in the United States. Kenneth R. Smith and David R. Bowling are affiliated with the School of Biological Sciences at the University of Utah, in Salt Lake City, Utah, in the United States. Jaret S. Reblin is affiliated with the Schiller Coastal Studies Center, at Bowdoin College, in Brunswick, Maine, in the United States. Andrew D. Richardson is affiliated with the Center for Ecosystem Science and Society and with the School of Informatics, Computing, and Cyber Systems at Northern Arizona University, in Flagstaff, Arizona, in the United States.

Abstract

Evergreen needleleaf forests (ENFs) play a sizable role in the global carbon cycle, but the biological and physical controls on ENF carbon cycle feedback loops are poorly understood and difficult to measure. To address this challenge, a growing appreciation for the stress physiology of photosynthesis has inspired emerging techniques designed to detect ENF photosynthetic activity with optical signals. This Overview summarizes how fundamental plant biological and biophysical processes control the fate of photons from leaf to globe, ultimately enabling remote estimates of ENF photosynthesis. We demonstrate this using data across four ENF sites spanning a broad range of environmental conditions and link leaf- and stand-scale observations of photosynthesis (i.e., needle biochemistry and flux towers) with tower- and satellite-based remote sensing. The multidisciplinary nature of this work can serve as a model for the coordination and integration of observations made at multiple scales.

Keywords: evergreen needleleaf forests, remote sensing, ecophysiology, ecosystem fluxes, photosynthesis

Evergreen needleleaf forests (ENFs) are one of the largest forest biomes in the world and are an important sink in the global carbon cycle (Smith et al. 2009). Notably, the carbon sequestration potential of ENFs is high, with an uptake of approximately 2 billion tons of carbon dioxide each year (Köhl et al. 2015). They also provide critical ecosystem services, including climate regulation, wildlife habitat, sustenance, and timber (Keenan et al. 2015, Felipe-Lucia et al. 2018). Anthropogenic climate change has shifted the baseline environmental conditions for ENFs, but the impacts of these changes on carbon budgets and ecosystem services remain uncertain (Liu et al. 2020a). Rising temperature and carbon fertilization have increased canopy greenness in some ENFs, suggesting enhanced potential for photosynthetic carbon uptake (Wang and Friedl 2019, Berner et al. 2020). However, the future of ENF carbon assimilation is threatened by a myriad of climate-related factors, including widespread drought (Bentz et al. 2019, Anderegg et al. 2020, Trugman et al. 2021), changes to growing season length, increased wildfire potential, and biotic agents of mortality (Anderegg et al. 2015, Kautz et al. 2017). In regions where warmer springs and drier summers are becoming more prevalent, ENFs have become more productive in the spring and less productive in the summer or fall, ultimately affecting long-term trends

in the seasonality, magnitude, and sign of net carbon exchange (Buermann et al. 2018, Fisher et al. 2018, Butterfield et al. 2020). Our understanding of the ENF carbon cycle is encumbered by limited observations of plant photosynthesis (i.e., carbon assimilation) at high spatiotemporal resolutions globally. Consequently, our predictions of the future carbon cycle remain highly uncertain, with some Earth system models suggesting that the terrestrial biosphere may even transition to a net carbon source by the end of the twenty-first century (Friedlingstein et al. 2022).

Optical remote sensing plays a critical role in detecting changes in evergreen photosynthesis and can provide an important constraint on our ability to predict and understand the future of ENFs (Schimel et al. 2019). Remote sensing can help scale leaf- and site-level observations across both space and time, enabling more robust quantification of ENF photosynthesis across the globe. Optical remote sensing is sensitive to both changes in plant physiology and the biophysics of how incident photons are reflected or emitted from vegetation (Zeng et al. 2022). The goal of this Overview is to review the fundamental biological and physical processes that inform the use of optical remote-sensing data for tracking photosynthesis in ENFs.

Received: March 22, 2023. Revised: October 31, 2023. Accepted: December 5, 2023

© The Author(s) 2024. Published by Oxford University Press on behalf of the American Institute of Biological Sciences.

All rights reserved. For permissions, please e-mail: journals.permissions@oup.com

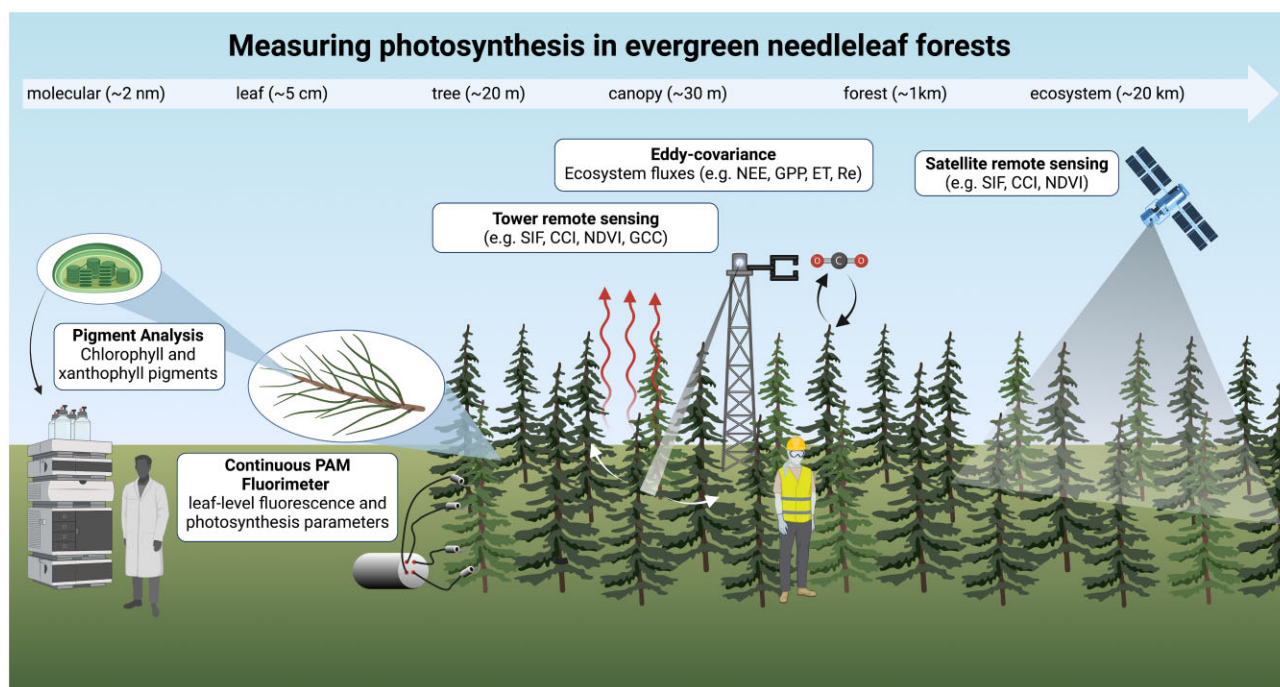


Figure 1. Summary of ways to measure evergreen needleleaf forest photosynthesis from the molecular to ecosystem scale and data types highlighted in this overview. Pigment analyses provides direct insight into light absorption and partitioning but has limited temporal resolution (samples must be collected and processed manually). Continuous pulse amplitude modulated fluorometry provides leaf-level information on the photosynthetic activity of plant photosystems, including information on the partitioning of light energy among different pathways. Tower-based remote sensing provides proxies for many variables related to photosynthetic carbon uptake, including forest chlorophyll and xanthophyll pigment content and net carbon uptake at a high spatiotemporal resolution (half-hourly, tree-canopy scale). Eddy-covariance-derived carbon-dioxide fluxes are the best available measure for carbon uptake via photosynthesis (gross primary production) at the canopy scale and can be derived at a half-hourly resolution. Satellite-based remote sensing is the only way we can detect photosynthesis at large spatial scales but is limited in its spatial and temporal resolutions. Illustration created with [BioRender.com](https://www.biorender.com).

We provide nonspecialists with an understanding of how these data can be used to better inform our understanding of the ENF carbon cycle. To do this, we use a suite of data (figure 1) collected from four ENF sites spanning a climate gradient across North America (figure 2). We begin by reviewing the mechanisms controlling the diurnal and seasonal dynamics of photosynthesis in ENFs and the physical and physiological controls on the fate of absorbed light at the leaf or needle level. These biological mechanisms are then scaled to the canopy level using a variety of different measurement approaches. We show how an integrated measurement approach can provide a more complete picture of carbon assimilation at the canopy scale. We further scale these measurements and their biological underpinnings to the biome level with satellite-based remote sensing. We end this Overview by discussing the need for multiscale and multidisciplinary research—spanning from leaf-level biology to physics and remote sensing—for advancing our understanding of the processes underpinning global change impacts on ENFs.

Needle-scale mechanisms controlling the daily and seasonal physiology of evergreen needleleaf forests

Photosynthesis uses light from the Sun to drive the conversion of carbon dioxide and water into energy-rich organic compounds (sugars and starch). Through this process, plants use solar power to sustain nearly all life on Earth. Light, temperature, nutrients, and the availability of water control photosynthesis (figure 3; Berry and Bjorkman 1980, Farquhar et al. 1980). Within a daily

cycle, a plant's ability to photosynthesize varies with changes in sunlight, temperature, and evaporative demand. Over days to weeks, plants acclimate to their environment and allocate resources to optimize photosynthesis during the active season, adjusting to seasonal changes (e.g., Logan et al. 1998, Huxman et al. 2003). To properly explain the mechanisms controlling the daily and seasonal photosynthetic physiology of ENFs, we begin by discussing the fate of sunlight.

Light travels from the Sun through Earth's atmosphere and into a forest canopy. Only a portion of the Sun's electromagnetic spectrum can be used to drive photosynthesis, known as *photosynthetically active radiation* (PAR; 400–700 nanometers [nm]). A portion of PAR is incident on soil, branches, and other nonphotosynthesizing media, whereas a fraction of this light ($fPAR_{chl}$) is absorbed by chlorophyll molecules in foliage and is known as *absorbed photosynthetically active radiation* ($APAR_{chl}$) such that

$$APAR_{chl} = fPAR_{chl} \times PAR \quad (1)$$

Chlorophyll molecules have a unique spectral signature in that they reflect more light in the green region of the spectrum and absorb strongly in the red and blue; therefore, plants appear green (Comar and Zscheile 1942). Optical metrics can approximate the fraction of light absorbed by chlorophyll ($fPAR_{chl}$) by probing the ratios of reflected light in the red, blue, and green spectral regions. Although $APAR_{chl}$ can vary seasonally because of changes in PAR, in ENFs with little understory, $fPAR_{chl}$ tends to remain seasonally constant (Steinberg et al. 2006, Serbin et al. 2013). This is because seasonal changes in chlorophyll content (figure 4; Magney et al. 2019) and canopy structure (Chen 1996) are small. Therefore, we

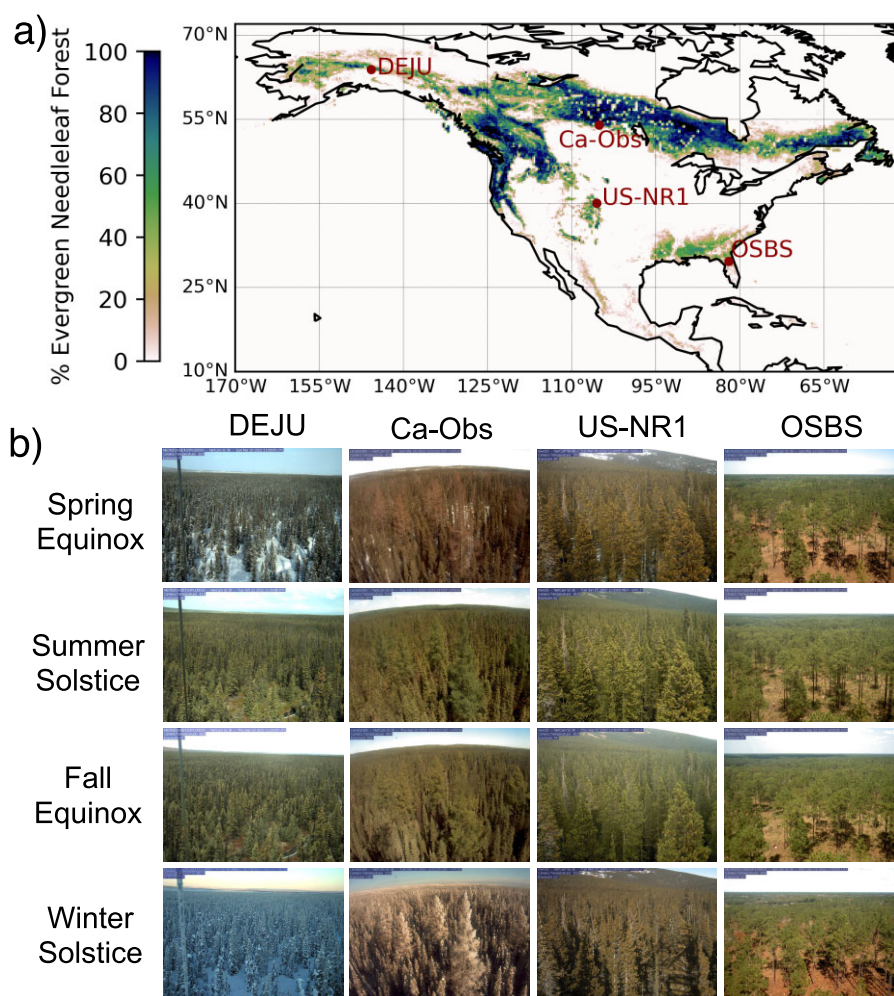


Figure 2. Overview of evergreen needleleaf forest (ENF) sites used in this overview. (a) The spatial extent and percentage cover of ENFs across North America, as well as the locations of the four field sites used in this study. The ENF percentage cover was derived from MODIS (the Moderate Resolution Imaging Spectroradiometer) International Geosphere-Biosphere Programme Land Cover 2019 data set at 500 meters resolution (Friedl and Sulla-Menashe 2019). The four sites include boreal forest locations in Alaska (DEJU, mean annual temperature = 0.4 degrees Celsius [°C], latitude = 63.9 degrees north [°N]) and Saskatchewan, Canada (Ca-Obs, 1.3°C, 54.0°N), a high elevation forest in Colorado (US-NR1, 2.8°C, 40.0°N), and a longleaf pine forest in Florida (OSBS, 21.1°C, 29.7°N). (b) Images of the four sites across seasons highlighting that canopy structure does not change with season in ENFs. Images: PhenoCam Network (<https://phenocam.nau.edu/webcam>), brightened for clarity.

cannot rely on optical metrics sensitive to $fPAR_{chl}$ alone and need to understand not just how much light is absorbed but also the fate of the energy of absorbed light.

When absorbing a photon, chlorophyll enters an excited state and will partition the energy to one of four potential pathways: photochemistry, damage via the formation of reactive oxygen species, thermal energy dissipation, and fluorescence (figure 3; Niyogi 1999). In order to maintain energy conservation, the yield of each pathway (ϕ) must add up to 1 such that

$$1 = \phi_P + \phi_D + \phi_N + \phi_F, \quad (2)$$

where ϕ_P is the yield of photochemistry, ϕ_D is the yield of damage, ϕ_N is the yield of thermal energy dissipation, and ϕ_F is the yield of fluorescence (Frankenberg and Berry 2018). The amount of photochemistry (which is linked to subsequent carbon uptake) a plant can perform depends on both the absorption of light by chlorophyll (i.e., $APAR_{chl}$) and the partitioning of light among these four pathways such that

$$\text{photosynthesis} \approx APAR_{chl} \times \phi_P. \quad (3)$$

Optical techniques can probe photosynthesis by approximating $APAR_{chl}$, ϕ_P , or both. Although ϕ_P cannot be directly observed with optical methods, we can rely on techniques that are sensitive to other pathways. Under typical environmental conditions, the damage pathway (ϕ_D) is negligible. Meanwhile, ϕ_N and ϕ_F tend to covary in predictable ways with ϕ_P in ENFs as a response to environmental controls (Frankenberg and Berry 2018). Much of our understanding of the partitioning of light among these pathways has come from pulse amplitude modulated (PAM) fluorometry (Maxwell and Johnson 2000). PAM fluorometry employs a pulsed measuring source of weak light, in combination with saturating pulses of light, measuring the subsequent fluorescence emissions to derive a variety of parameters that can tell us about photochemical performance and how light energy is being partitioned (we refer readers to Schreiber 2004 for details on PAM fluorometry). By understanding how ϕ_N and ϕ_F pathways operate in ENFs, we can relate the biology of photochemistry (ϕ_P) to what can be detected with optical methods.

The dynamics of ENF photosynthesis are unique, because they absorb light year-round, but they can experience seasonal stress, hampering their ability to perform photosynthesis. For

Mechanisms controlling diurnal and seasonal dynamics of photosynthesis

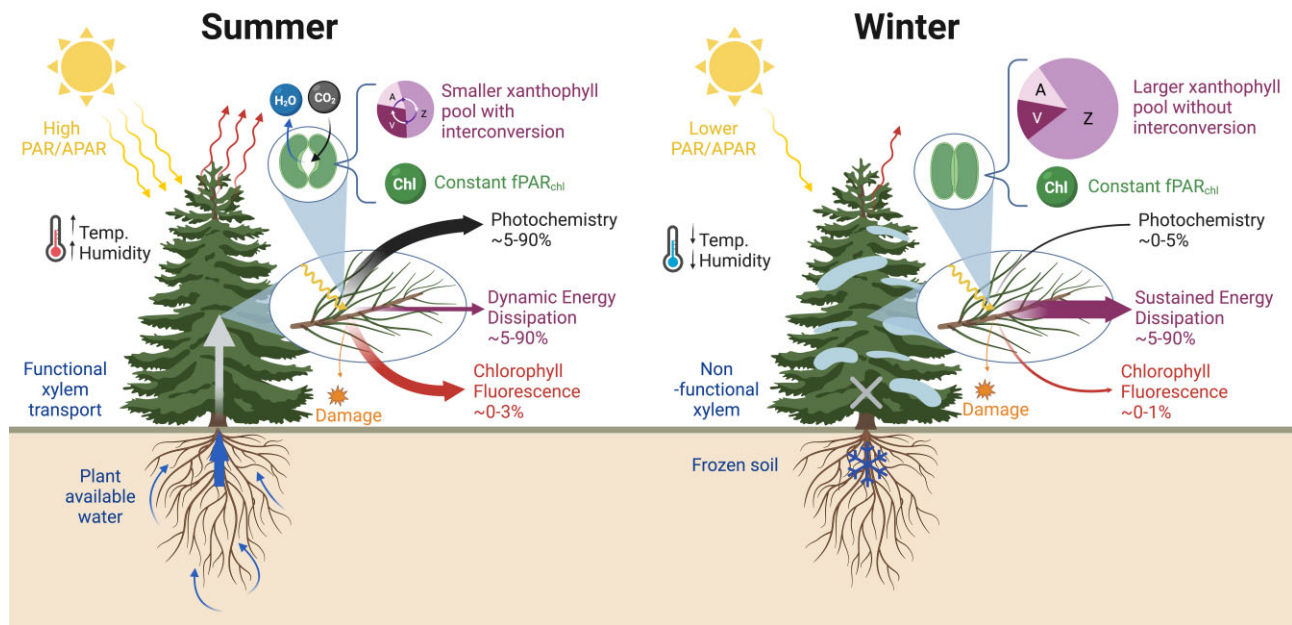


Figure 3. Overview of the mechanisms controlling the daily and seasonal physiology of evergreen needleleaf forests (ENFs), as well as their environmental controls. The summer and winter examples highlight the biological mechanisms associated with most extreme environmental conditions ENFs experience at higher latitudes and altitudes. Illustration created with [BioRender.com](https://www.biorender.com).

example, subzero temperatures in winter (e.g., NEON's Delta Junction site [DEJU] in Alaska, the Saskatchewan-Western Boreal, Mature Black Spruce site [Ca-Obs] in Canada, and the Niwot Ridge site [US-NR1] in Colorado) inhibit enzyme activity and drive a lack of liquid water availability due to ice forming in the soil, within the roots, the trunk, and the distal stems (figure 3; Sevanto et al. 2006, Bowling et al. 2018, Pierrat et al. 2021, Nehemy et al. 2022). Repeated freeze-thaw events can also lead to damage to the water transport pathway via embolism of xylem (Sperry and Sullivan 1992). Because of the combination of cold temperature stress and water limitation, although they are still absorbing light, many plants in cold locations down regulate the biochemical processes of photosynthesis during winter (figure 3; Adams et al. 2004). Because absorbed light energy cannot be efficiently used for photochemistry, it must be sent down alternative energy pathways.

When a plant absorbs more light than can be used to drive photochemistry (ϕ_p), the excess energy can damage the plant's tissue. Excited chlorophyll molecules can pass energy to oxygen, transforming it into singlet oxygen (Niyogi 1999). This is an unstable form in the family of reactive oxygen species, which can irreversibly modify proteins, membrane lipids, and chlorophyll itself, potentially setting off a cascade of harmful cellular oxidation reactions (Logan 2006). Singlet oxygen formation via energy transfer from chlorophyll is a low-probability biophysical event (i.e., $\phi_D \approx 0$ for healthy plants); however, it can occur at appreciable and problematic levels when chlorophyll molecules remain in the excited state when photochemistry is unable to claim that energy. It is advantageous, then, for plants to have systems in place to deal with light absorbed in excess of what can be used to perform photochemistry.

All plants possess a well-regulated pathway to safely divert excess absorbed light energy as heat (Demmig-Adams and Adams 2006). This pathway, known as *thermal energy dissipation*, is

modulated by three xanthophyll pigment molecules, zeaxanthin (Z), antheraxanthin (A), and violaxanthin (V), which interconvert through a process known as the *xanthophyll cycle* (Demmig-Adams and Adams 2006). Z and A undergo exothermic chemical reactions, which facilitate the conversion of excitation energy into heat that can be dissipated to the surrounding environment (Holt et al. 2004, Holzwarth and Jahns 2014). The portion of light energy dissipated via this pathway (ϕ_N) is controlled by the ratio of Z + A to chlorophyll. This ratio is modulated via enzyme-catalyzed interconversions between Z, A, and V; the latter pigment is unable to carry out energy dissipation (Niyogi et al. 1998). When temperature allows enzymatic activity (i.e., during the warm season), plants interconvert xanthophyll pigments to dissipate light absorbed in excess (figure 3; Demmig-Adams and Adams 1992). This type of dynamic thermal energy dissipation happens over shorter periods of time, from minutes to hours, and can help plants prevent damage during short-term stress and routine absorption of light in excess (e.g., midday).

ENFs also use a form of sustained thermal energy dissipation over winter (Demmig-Adams and Adams 1992, Huner et al. 1993). Because low temperature inhibits enzyme-catalyzed interconversion of xanthophyll cycle pigments, evergreens retain high levels of Z + A over winter in relation to the total xanthophyll pool (V + A + Z; figure 3; Verhoeven 2014). This induces a sustained form of thermal energy dissipation marked by an increase in $(Z + A) \div (V + A + Z)$ evident in winter dormant ENFs (DEJU and US-NR1 in figure 4a,b). In addition to the change in xanthophyll pigment ratios, ENFs also increase the total amount of xanthophyll pigments, which is most often quantified as the ratio between chlorophyll and carotenoid pigments (including xanthophylls). Winter dormant ENFs therefore exhibit a decrease in chlorophyll or carotenoid ratios over winter (figure 4a,b). ENFs experiencing mild winters (e.g., the OSBS [Ordway-Swisher Biological Station] site in Florida) have little need for sustained

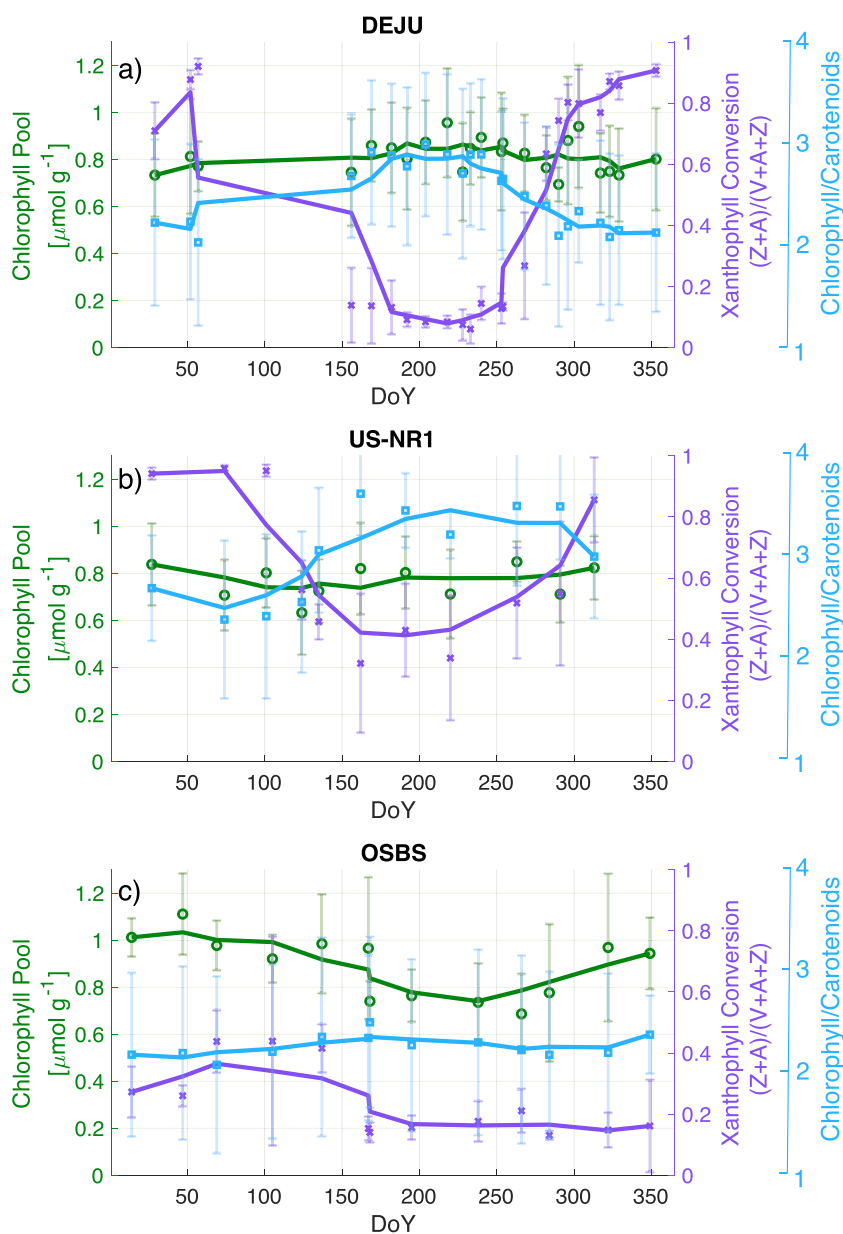


Figure 4. Pigments collected from (a) DEJU, (b) US-NR1, and (c) OSBS field sites. The chlorophyll pool remains relatively constant year-round at all three sites (DEJU, US-NR1, and OSBS). The relatively cold sites (DEJU and US-NR1) exhibit much larger seasonal variability in xanthophyll conversion state than the warm site (OSBS). Pigment analysis is performed by collecting needle tissue from 8–10 different trees at each site, immediately flash-frozen in liquid nitrogen and stored in a freezer at -80 degrees Celsius until analysis. Pigments are then extracted in acetone and analyzed by HPLC as described in Bowling and colleagues (2018). At DEJU, 10 samples were collected from 10 different trees approximately every 2 weeks from August 2019 to November 2020. At US-NR1, approximately 30 samples were collected from approximately 18 different trees from July 2017 to June 2018. At OSBS, five samples were collected from five different trees from June 2020 to June 2021. The plotted points indicate the average value of all pigment samples on a collection day, and the error bars indicate the standard deviation of the sample values.

energy dissipation, and therefore do not exhibit dramatic seasonal variation in pigment pools (figure 4c). Because the yield of photochemistry (ϕ_P) depends on the yield of thermal energy dissipation (ϕ_N ; equation 2; Porcar-Castell et al. 2014) and because ϕ_N is primarily modulated by xanthophyll pigment concentrations, we can use the spectral signatures of xanthophyll pigments to probe photosynthesis.

The final path for the energy of excited chlorophyll is fluorescence emission (ϕ_F ; figure 3). Excited chlorophyll can fall back to its unexcited state with the emission of a red or near infrared photon—that is, fluorescence. The intensity of the fluorescence emission is therefore a function of APAR_{chl} , and the yields of

alternative energy partitioning pathways. Fluorescence never accounts for more than a small fraction (typically 1%–3%) of APAR_{chl} and is not a method for plants to safely dissipate appreciable excess energy. Rather, it is a byproduct of chlorophyll excited electrons falling back to their ground state and varies in predictable ways with ϕ_P , depending on the light environment. Under extremely low-light conditions, such as dusk and dawn, photosynthesis is typically limited by the amount of light absorbed rather than biochemical capacities. Under light-limited conditions, light energy is therefore almost entirely sent down the photochemistry pathway (known as the *photochemical quenching* [PQ] phase), with essentially no energy being dissipated as heat ($\phi_N \approx 0$).

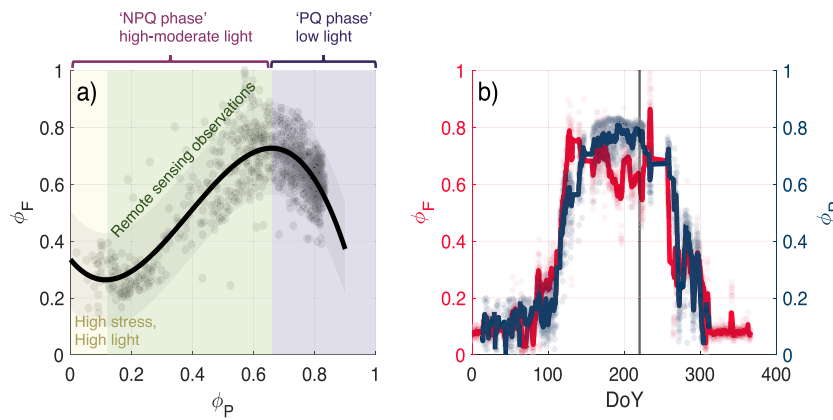


Figure 5. Continuous pulse amplitude modulated (PAM) measurements made at DEJU. (a) The relationship between normalized steady state fluorescence yield (ϕ_F) and photosystem II yield (ϕ_P) during the warm season (Day of year, DoY, 100–250) fit with a third order polynomial showing 95% confidence intervals. The data are in strong agreement with the theorized relationship from Magney and colleagues (2020) and the observed relationship in Maguire and colleagues (2020). We observe an inverse relationship under low-light conditions and a direct relationship under moderate light conditions, where remote sensing observations are typically made. (b) Seasonal covariation between ϕ_F and ϕ_P . The PAM measurements were recorded every 10 seconds with a saturating pulse every 2 hours using a Walz monitoring PAM (MONI-PAM). MONI-PAM heads were affixed to four needle clumps on the branches of three different trees, facing all cardinal directions. The data were averaged on a 2-hourly basis from August 2021 through fall 2022.

During the PQ phase, the yields of photochemistry (ϕ_P) and the yields of fluorescence (ϕ_F) will exhibit an inverse relationship (figure 5a, equation 3; Porcar-Castell et al. 2014, van der Tol et al. 2014, Magney et al. 2020, Maguire et al. 2020). Under moderate or typical-light conditions, thermal energy dissipation mechanisms (ϕ_N , known as the *nonphotochemical quenching* [NPQ] phase) regulate the amount of light used for photochemistry. Because ϕ_N pulls energy away from ϕ_P and ϕ_F , during the NPQ phase, ϕ_P and ϕ_F exhibit a positive relationship (figure 5a; Porcar-Castell et al. 2014, van der Tol et al. 2014, Magney et al. 2020, Maguire et al. 2020). In ENFs where seasonal changes in sustained thermal energy dissipation (ϕ_N) drive changes in ϕ_P and ϕ_F (Porcar-Castell 2011), we observe strong covariation between the seasonal cycles of ϕ_P and ϕ_F (figure 5b). Remote-sensing observations of fluorescence also typically occur under NPQ phase conditions and can serve as a robust proxy for photosynthesis when averaged over longer temporal scales (i.e., seasonally, Magney et al. 2020).

Canopy-scale measures of photosynthesis and remote-sensing proxies

Carbon uptake via photosynthesis can be studied at the canopy scale with instruments mounted above the vegetation on towers using the eddy covariance technique (for a review, see Baldocchi 2020). This technique uses high-frequency observations of atmospheric turbulence, temperature, and gas concentrations (typically, carbon dioxide and water) to derive vertical fluxes of carbon, water, and heat (sensible and latent) between a forest and the atmosphere within a varying footprint range around the tower. The eddy covariance technique provides a measure of the net carbon dioxide flux (net ecosystem exchange), which is the combination of carbon dioxide uptake by photosynthesis (gross primary production [GPP]) and the release of carbon dioxide through respiration (ecosystem respiration). Net ecosystem exchange can be split into its component parts (GPP and ecosystem respiration) using a wide variety of models based on a combination of temperature, sunlight, and evaporative demand (Reichstein et al. 2005, Desai et al. 2008, Lasslop et al. 2010, Tramontana et al. 2020), all of which carry uncertainties (Papale et al. 2006, Wutzler et al. 2018).

Carbon uptake via photosynthesis at the canopy scale can be described using the light-use efficiency model of GPP (Monteith 1972, 1977):

$$\text{GPP} = \text{PAR} \times f\text{PAR}_{\text{chl}} \times \text{LUE}_P, \quad (4)$$

where LUE_P is the light-use efficiency of photosynthesis at the canopy scale (canopy level ϕ_P). As at the leaf level, GPP is dependent on light ($\text{APAR}_{\text{chl}} = \text{PAR} \times f\text{PAR}_{\text{chl}}$), temperature, and the availability of water (both of which will affect LUE_P ; Luysaert et al. 2007, Beer et al. 2010). This is observed across our four study sites. The first three sites (DEJU, Ca-Obs, and US-NR1) experience cold winters with subzero temperatures (figure 6a–d) but differ in the amount of light they receive (figure 6e–h). During winter, these cold weather sites are photosynthetically dormant (slightly positive net ecosystem exchange, no GPP; figure 6i–p) and therefore use the thermal energy dissipation pathway (ϕ_N) to dissipate excess energy. This results in a seasonal cycle in LUE_P (figure 6q–t) where plants can safely divert excess energy from sunlight while remaining photosynthetically dormant. The extent to which ϕ_N is necessary to prevent damage also depends on the intensity of the light over winter. Specifically, the high elevation of US-NR1, in Colorado, ensures a cold winter—despite the lower latitude—resulting in dramatically higher PAR in the winter than that at the more northerly sites. This combination amplifies the need for sustained thermal energy dissipation in comparison with more high-latitude sites. The warmest site, OSBS, in Florida, photosynthesizes year-round and therefore does not employ sustained energy dissipation. On the basis of the light-use efficiency model, canopy-level remote-sensing metrics for tracking photosynthesis are typically sensitive to either $f\text{PAR}_{\text{chl}}$ or approximate LUE_P on the basis of the partitioning of energy into thermal dissipation (ϕ_N) or fluorescence (ϕ_F) pathways.

Reflectance-based vegetation indices are the most common type of optical measure capable of tracking changes in photosynthesis. These are typically calculated using a normalized difference formula:

$$\text{Index} = \frac{\rho_1 - \rho_2}{\rho_1 + \rho_2}, \quad (5)$$

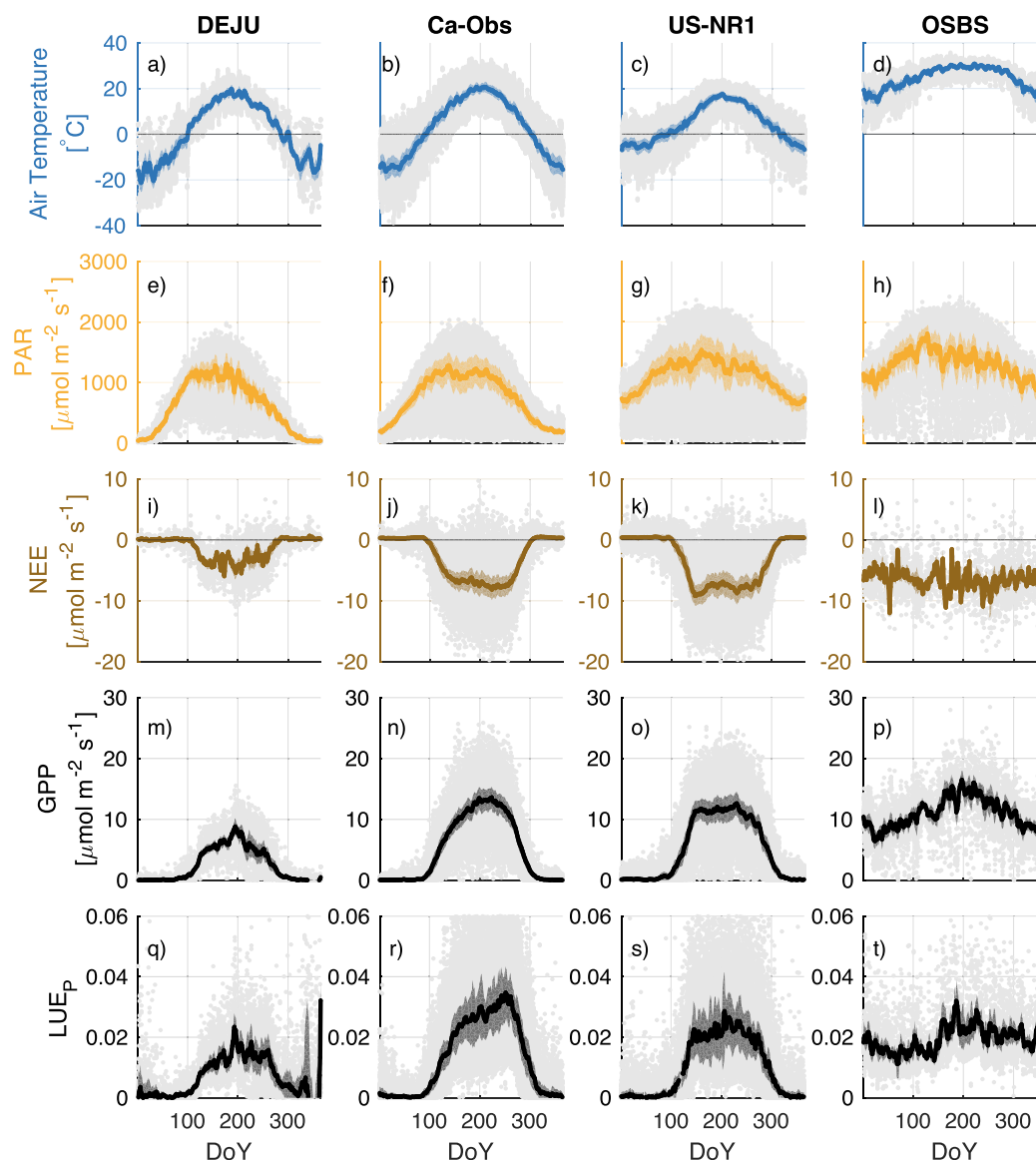


Figure 6. Midday (10:00–14:00) stand-level (a)–(d) air temperature, (e)–(h) PAR, (i)–(l) net ecosystem exchange, (m)–(p) GPP, and (q)–(t) LUE_P data from the four field sites. LUE_P is approximated by assuming $fPAR \approx 0.5$ and seasonally invariant; therefore, $LUE_P = GPP \div (PAR \times 0.5)$. The dots are individual data points, the colored lines are the average interannual midday values, and the shaded regions are the interannual midday standard deviation. Meteorological data were collected at DEJU from January 2017 to July 2022, at Ca-Obs from January 1999 to December 2021, at US-NR1 from January 1998 to December 2021, and at OSBS from December 2016 to July 2022.

where 1 and 2 are reflectance in the wavelength bands of interest. The first of these reflectance-based metrics to be widely used was the normalized difference vegetation index (NDVI; Tucker 1979). NDVI takes advantage of the difference in reflectance between the red (sensitive to chlorophyll absorption; approximately 620–670 nm) and near infrared (approximately 830–860 nm) regions of the spectrum (figure 7; Tucker 1979). It provides a good measure of canopy structure, particularly the presence or absence of chlorophyll (figure 8a–d) and, therefore, $fPAR_{chl}$. The sensitivity of NDVI to $fPAR_{chl}$ means that NDVI is a good proxy for GPP in systems where changes in $fPAR_{chl}$ are significantly greater than changes in LUE_P (equation 4), and therefore, canopy structure and carbon uptake are closely linked (e.g., crops, deciduous ecosystems). However, it fails to detect changes in GPP in ENFs due to minimal seasonal change in canopy chlorophyll content, and therefore $fPAR_{chl}$

(Magney et al. 2019, Pierrat et al. 2022a). In addition, NDVI is highly sensitive to the presence of snow cover because of the large difference in reflectance between vegetation and snow in the near infrared (figure 7, figure 8a–d; Myers-Smith et al. 2020, Wang et al. 2023). This complicates the interpretation of NDVI in ENFs, which are commonly affected by snow contamination within the sensor field of view. Derivations of NDVI that also use the difference between the red and near infrared regions of the spectrum, such as the near-infrared reflectance of vegetation (NIRv; Badgley et al. 2017, 2019) and the enhanced vegetation index (EVI), among others, have been able to account for background and soil contamination but still fail to capture changes in photosynthetic phenology of ENFs due to the decoupling between chlorophyll content and photosynthesis (Sims et al. 2006, Garbulsky et al. 2010, Gamon et al. 2013).

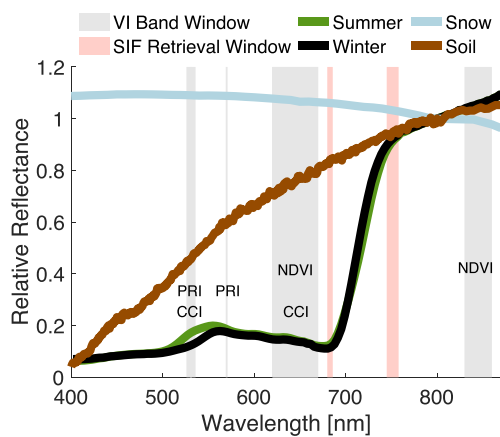


Figure 7. Spectral regions where reflectance-based vegetation indices are commonly calculated (shaded gray), SIF retrievals are commonly performed (shaded red), and example reflectance data of vegetation and snow normalized at 800 nanometers. Vegetation reflectance data are from US-NR1 and processed following Cheng and colleagues (2020). The snow and soil reflectance data are from the Advanced Spaceborne Thermal Emission and Reflection Radiometer Spectral Library (Baldrige et al. 2009, Meerdink et al. 2019).

Reflectance-based indices that are sensitive to xanthophyll pigment activity in ENFs have shown a marked improvement in tracking the photosynthetic phenology of ENFs over greenness-based metrics. This is because xanthophyll pigment activity modulates how much light energy is sent down the thermal energy dissipation pathway (ϕ_N), which can inform LUE_P or ϕ_P . The first of these to be developed, the photochemical (or physiological) reflectance index (PRI), exploits a narrow band at 531 nm (which is sensitive to the conversion state of xanthophyll cycle pigments) in reference to a narrow band at 570 nm (which does not change with xanthophyll interconversion; Gamon et al. 1992, 1997). This is noticeable in the difference in reflectance spectra in the 531 nm region from the US-NR1 site (figure 7) between summer (when Z concentrations are lower) and winter (when Z concentrations are higher). Over short temporal scales (e.g., over the course of a day in the growing season), PRI is sensitive to rapidly reversible thermal energy dissipation dynamics (ϕ_N) in ENFs, making it effective for tracking diurnal changes in LUE_P (Gamon et al. 2015, Yang et al. 2020). Over longer temporal scales (seasons), PRI is sensitive to sustained thermal energy dissipation because of winter increases in Z + A pigments (figure 8e–h; Wong and Gamon 2015a, 2015b). PRI is also highly sensitive to the presence of snow on the canopy, which presents a significant challenge in ENFs. It is also not presently measured from spaceborne platforms. The best available satellite proxy for PRI, the chlorophyll-carotenoid index (CCI), was specifically developed to track the seasonal changes in the ratio of chlorophylls to carotenoids (including xanthophyll pigments) using reflectance bands from the Moderate Resolution Imaging Spectroradiometer (MODIS, band 11 at 526–536 nm and band 1 at 620–670 nm; Gamon et al. 2016). By tracking the ratio of chlorophylls to carotenoids, CCI is also able to track sustained energy dissipation in ENFs (figure 8i–8l) and is therefore a good proxy for ENF carbon uptake (Gamon et al. 2016, Wang et al. 2023).

In addition to reflectance-based metrics that employ narrow wavelength bands, digital repeat photography can be used to track seasonal changes in canopy color and, therefore, the photosynthetic phenology of ENFs. Specifically, the green chromatic coor-

dinate (G_{CC}) can be calculated from images as

$$G_{CC} = \frac{G}{R + G + B}, \quad (6)$$

where G, R, and B are the mean intensity of the green, red, and blue color channels (Richardson 2019). Prior work has shown that G_{CC} is sensitive to the changes in canopy color associated with variation in leaf pigment ratios (including the ratio of chlorophyll to xanthophyll pigments) in ENFs (Seyednasrollah et al. 2021). Because of this sensitivity, G_{CC} can probe thermal energy dissipation, and therefore tracks the seasonality of GPP. Start of season and end of season transition dates derived from G_{CC} are well aligned with start of season and end of season transition dates derived from eddy-covariance GPP as well as the onset of transpiration, as was determined by stem-radius measurements in ENFs (Seyednasrollah et al. 2021, Nehemy et al. 2023). G_{CC} from our four experimental sites shows good agreement with the seasonal cycle of GPP but does not show a consistent ratio between G_{CC} and GPP (figure 8m–p). Snow cover affects G_{CC} values by obscuring the canopy in the region of interest and making it less green, but the values only shift down by approximately 10% (Seyednasrollah et al. 2021). A major advantage of G_{CC} is the ease of measurement at the canopy scale and the accessibility of images and data from 600 sites globally with a standardized processing approach through the PhenoCam Network (Richardson et al. 2018). This level of standardization and accessibility is currently unavailable for most other canopy-level remotely sensed data.

Another approach to probe photosynthesis remotely is the use of the fluorescence emitted by excited chlorophyll. Under natural sunlight conditions, this is referred to as *sun- or solar-induced chlorophyll fluorescence* (SIF). SIF has been shown significant potential for tracking GPP in ENFs (figure 8q–t; Magney et al. 2019, Pierrat et al. 2021, 2022a, 2022b). Canopy-level SIF is expressed similarly to GPP (equation 4) using the light-use efficiency model as

$$SIF = PAR \times fPAR_{chl} \times LUE_F \times f_{esc}, \quad (7)$$

where LUE_F is the light-use efficiency of fluorescence (ϕ_F integrated over all leaves or needles within the sensor field of view) and f_{esc} is the fraction of SIF photons that escape the canopy and reach the detector. We can relate SIF and GPP by combining equations (5) and (8):

$$GPP = SIF \times \frac{LUE_P}{LUE_F \times f_{esc}}. \quad (8)$$

SIF and GPP are therefore linked by both shared drivers ($APAR_{chl} = PAR \times fPAR_{chl}$), as well as leaf-level biological parameters (ϕ_P and ϕ_F) calculated at the canopy level (LUE_P and LUE_F). Under typical conditions for remote-sensing observations, when thermal energy dissipation regulates photochemistry (the NPQ phase) leading to covariation between ϕ_P and ϕ_F (figure 5a) and f_{esc} is invariant, the $LUE_P \div (LUE_F \times f_{esc})$ term becomes approximately constant. This leads to a linear relationship between SIF and GPP (Sun et al. 2018). Therefore, SIF closely tracks both the seasonality (figure 8q–t) and diurnal dynamics of GPP across a variety of ecosystems (Yang et al. 2015, Magney et al. 2019, He et al. 2020, 2020, Pierrat et al. 2022a). Furthermore, because SIF is an emitted signal and not a reflectance-based metric, it is less sensitive to the presence of snow (figure 8q–t) and cloud cover (Frankenberg et al. 2011, Mohammed et al. 2019, Chang et al. 2020). The ability to use

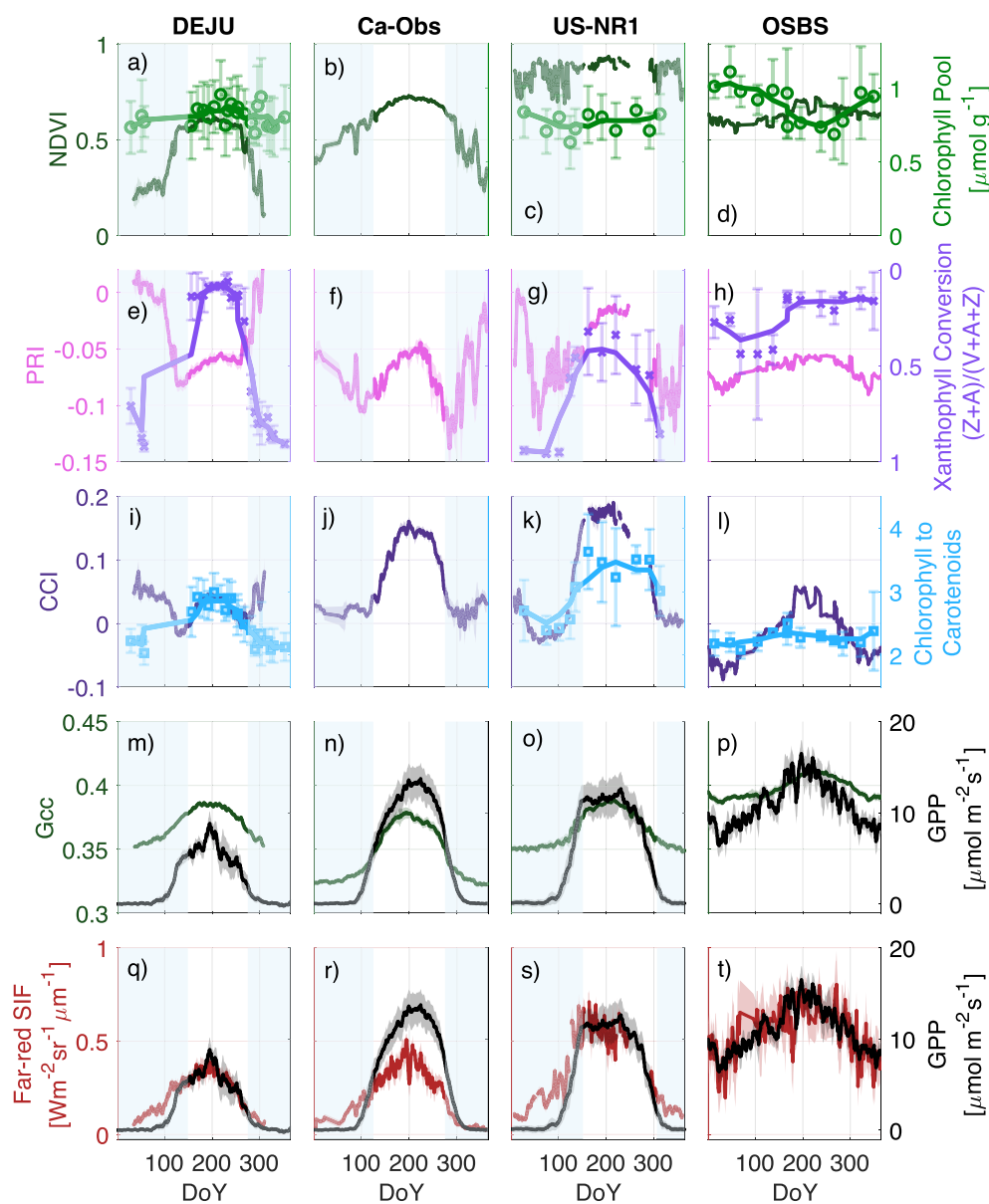


Figure 8. Tower-based remote sensing combined with leaf-level pigment data and eddy-covariance derived GPP. (a)–(d) NDVI and chlorophyll concentration, (e)–(h) PRI and xanthophyll conversion state, (i)–(l) CCI and chlorophyll to carotenoid ratio, (m)–(p) G_{cc} and GPP, and (q)–(t) SIF and GPP. NDVI, PRI, CCI, and SIF data were collected using PhotoSpec. The additional measurement and data processing details from PhotoSpec can be found in Grossmann and colleagues (2018), Magney and colleagues (2019), Pierrat and colleagues (2022a, 2022b). The PhotoSpec data were collected at DEJU from August 2019 to September 2021, at Ca-Obs from August 2019 to December 2021, at US-NR1 from June 2017 to June 2018, and at OSBS from June 2021 to July 2022. The G_{cc} data were obtained from the PhenoCam Network (<https://phenocam.nau.edu/webcam>). The plotted lines represent average interannual midday (10:00–14:00) values, and the shaded regions are the interannual midday standard deviation. The vertically shaded regions indicate days where snow on the canopy obscures remote sensing observations.

SIF as a proxy for GPP in ENFs has led to substantial advances in our understanding of ENF carbon dynamics.

Studies at fine spatiotemporal resolutions (leaf and tower) have highlighted nuance to the SIF–GPP relationship that can be attributed to a combination of decoupling between ϕ_P and ϕ_F (and subsequently LUE_P and LUE_F) modulated by thermal energy dissipation dynamics (figure 5a; Magney et al. 2020, Maguire et al. 2020, Marrs et al. 2020, Pierrat et al. 2022a), and variation in f_{esc} . In ENFs with strong seasonal temperature variations, such as DEJU, Ca-OBS, and US-NR1, the GPP–SIF relationship changes throughout the year because of sustained energy dissipation dynamics. In addition, in winter when photochemistry is strongly downregulated at these sites, SIF still exhibits a small light response when GPP

is absent, which leads to a nonzero SIF signal and an increase in SIF prior to changes in GPP (figure 8q–t; Magney et al. 2019, Yang et al. 2022, Pierrat et al. 2022a). The winter SIF light response can be explained as persistent photosystem activity that does not reflect carbon assimilation (i.e., zero $\phi_P \div LUE_P$ and nonzero $\phi_F \div LUE_F$). The nuances in the SIF–GPP relationship does not preclude the use of SIF as a proxy for GPP, but they do motivate future work to understand when and where divergence between SIF and GPP occurs and how we can best account for it.

Given that remote-sensing metrics can contain information on both plant structure ($fPAR_{chl}$, f_{esc}) and function (light partitioning among ϕ_P , ϕ_N , and ϕ_F), combining multiple metrics can help paint a more complete picture of ENF photosynthesis. Specifically,

combining SIF with reflectance-based indices improves our ability to predict GPP beyond the use of any one metric alone (Wang et al. 2020, Hikosaka and Tsujimoto 2021, Kováč et al. 2022, Wong et al. 2022, Pierrat et al. 2022b). This can be attributed to the fact that although some metrics are sensitive to similar physical parameters ($fPAR_{chl}$, f_{esc}), they describe different physiological parameters; that is, reflectance-based metrics are sensitive to leaf or needle composition that controls thermal energy dissipation (ϕ_N), whereas SIF depends on fluorescence yields (LUE_F and ϕ_F). In combination, these metrics provide a more complete description of the fate of photons absorbed by canopies. Both statistical (Zeng et al. 2019, Liu et al. 2020b, Wong et al. 2022) and machine learning approaches (Cheng et al. 2020, Bai et al. 2022, Pierrat et al. 2022b) have been used to incorporate information from both SIF and vegetation indices to predict GPP. There is not yet a universal quantitative framework for relating these metrics because intersensor differences and footprint-mismatch make cross-comparison between sites and data sets difficult (Gamon 2015). A more integrated network of sensors would significantly advance our ability to develop universal quantitative relationships. Despite these limitations, combining SIF with vegetation indices typically results in improved predictive capacity for GPP over any single metric alone (Pierrat et al. 2022b).

Global-scale satellite remote sensing of evergreen needleleaf forests

The high cost of flux tower observations and restrictions on site suitability limit the locations where eddy covariance and other canopy-scale measurements can be applied. Although drone and airborne observations can scale site-level observations over a larger area, to scale broadly across the terrestrial land surface, satellite remote-sensing observations are necessary (Jung et al. 2011, 2020, Zeng et al. 2022). Satellite remote-sensing products (e.g., NDVI, CCI, SIF) are sensitive to the same underlying physical and physiological processes that can be measured at the leaf or needle and site levels but offer expanded spatiotemporal monitoring of vegetation (Schimel et al. 2015, Zeng et al. 2022). The spatial resolutions of satellite products range from meters to kilometers and temporal resolutions from subdaily (geostationary) to daily and more than 8 days (global coverage) depending on platform. Satellite observations offer applications for monitoring and understanding both short (diurnal, seasonal) and long term (annual, decadal) dynamics of whole landscape or biome processes at a spatial scale much broader than a single site. Some satellite missions also offer long-term data availability with certain missions dating as far back as the 1970s (e.g., Landsat, Xiao et al. 2019). Long-term satellite records have been used to evaluate changes in annual carbon uptake (Myneni et al. 2001, Dong et al. 2003) and phenology (Zhang et al. 2003, White et al. 2009, Keenan et al. 2014). In addition, monitoring ecosystem function from space has applications for assessing long-term trends in forest stress severity and recovery (e.g., fires, pests, drought; French et al. 2008, Eklundh et al. 2009, Beck et al. 2011, Michaelian et al. 2011). The expansion of the spatiotemporal range that satellite data provides, however, typically comes at the expense of spatiotemporal resolution. Therefore, it is necessary to consider both the spatial and temporal scaling benefits and limitations of satellite data.

Satellite reflectance-based metrics, such as NDVI from MODIS and Landsat have been used for many years to monitor the global biosphere. For example, maps of NDVI reveal the spatial and seasonal variation of ecosystem structure across North America

(figure 9a,b). However, care has to be taken with these observations, because satellites aggregate optical signals from multiple sources in a given area, often called *ground pixel*, into a single measurement (Zeng et al. 2022). This makes interpretation of reflectance-based observations challenging in structurally complex and heterogeneous ecosystems such as ENFs with multiple overstory species and contributions from understory vegetation, soil, and snow (Maguire et al. 2021). Mixed forest sites contain evergreen and deciduous trees with contrasting adaptive strategies (e.g., phenology, photosynthetic capacity; Givnish 2002)—also complicating the seasonal interpretation of satellite data. Depending on the dominant vegetation type, satellite remote sensing may be biased to the dominant optical signal on the basis of density and leaf area (Atherton et al. 2017, Pierrat et al. 2021). In sparse canopies, understory plants, rock, and soil affect reflectance-based indices such as NDVI. For this reason, correction factors (Eitel et al. 2006) or other vegetation indices (e.g., EVI and NIRv) are useful in minimizing the influence of understory components. Reflectance-based metrics are also highly sensitive to cloud cover, which may contaminate observations, even for partial cover in a pixel, leading to data gaps (Walther et al. 2016, Cheng et al. 2022). Finally, the sensitivity of reflectance-based metrics to snow (figure 7) can lead to a seasonal signal in reflectance-based metrics that is not associated with changes in photosynthetic phenology. This is noticeable across three of our study sites (figure 9e–g). Correction approaches (e.g., Wang et al. 2023) may help remove the impact of snow on vegetation indices but this has yet to be widely adopted. Despite these limitations, global reflectance based remote-sensing products have successfully been used to parameterize and constrain model predictions of carbon uptake (Gonsamo et al. 2012, Smith et al. 2020), monitoring and managing change at large scales (Zeng et al. 2022), and remain one of our most important tools to reduce uncertainties in future climate predictions (Friedlingstein et al. 2014).

The measurement of SIF from space has led to considerable advances in monitoring ENF photosynthesis in recent years. Because of the underlying physical ($APAR_{chl} = PAR \times fPAR_{chl}$, f_{esc}) and physiological drivers (LUE_F) of SIF, it can reveal the spatial and seasonal variation of ecosystem structure and function across North America (figure 9c–h). Satellite SIF observations across our study sites (figure 9e–h) show a comparable seasonal cycle to tower-based SIF and eddy-covariance GPP (figure 8q–t), illustrating the potential of satellite SIF observations over larger spatial scales. As an emitted signal, SIF has a lower sensitivity to cloud (Frankenberg et al. 2014, Doughty et al. 2019, Guanter et al. 2021) and snow cover (Luus et al. 2017), therefore making it more robust across the seasons (figure 9e–g). This is especially important during the onset of photosynthesis, which often coincides with the snowmelt period (Pierrat et al. 2021). SIF has also shown significant potential for detecting the impacts of drought, even before changes in canopy greenness (NDVI) are detected (Shen et al. 2021, Mohammadi et al. 2022). This enables potentially real-time evaluations of ecosystem health. In analogy with tower-based results, combining satellite SIF with reflectance-based metrics has the potential to overcome many of the limitations presented by any individual metric alone; however, this has yet to be fully investigated.

Integrating satellite products from different sensors should also be considered with care, because overpass time and pixel locations may not align temporally and spatially, leading to spatiotemporal mismatch (Gao et al. 2006, Alcaraz-Segura et al. 2010). In addition, the seasonal variation in solar radiance and high solar-zenith angles results in unequal availability of satellite data between winter and summer (figure 9a–d), which may bias

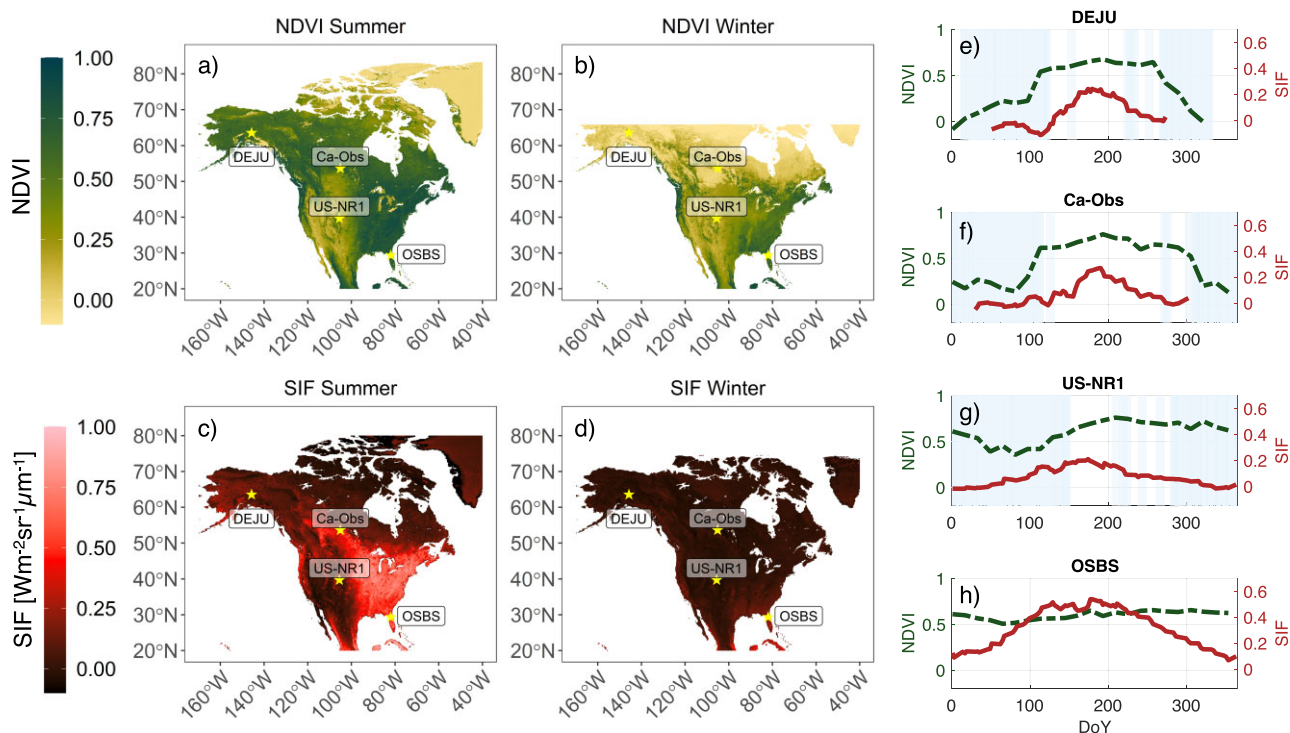


Figure 9. (a)–(d) Average summer (June–September) and winter (December–March) MODIS NDVI and TROPOMI SIF. The yellow stars represent site locations. (e)–(h) 16-day MODIS NDVI (unitless) and 16-day daily corrected TROPOMI SIF (in watts per square meter per steradian per micrometer) both averaged annually from 2018 to 2021. The vertically shaded regions indicate days with snow present based on daily MODIS NDSI. The winter maps show limited spatial coverage of the northern extent due to high solar zenith angles leading to inadequate solar irradiation.

interpretation of the seasonality of photosynthesis. Forests at higher latitudes will also be more sensitive to sun-sensor geometry, requiring postprocessing steps such as bidirectional reflectance distribution function and atmospheric corrections (Asner 1998).

Satellites offer data sets that expand the spatiotemporal range of tower-based observations. Despite the challenges imposed by mixed pixels and snow and cloud contamination, satellites are essential tools to better monitor ENFs and to inform global carbon models. More research is needed to fully understand and interpret satellite-based data products for tracking photosynthesis in ENFs. There remains a need for mechanistic validations at a high spatiotemporal resolution (Nelson et al. 2022) with measurements such as those discussed earlier.

Multiscale observations for an integrated understanding of evergreen needleleaf biology

Climate change is likely to have complex and multifaceted impacts on ENF photosynthesis, which could alter the structure, composition, and productivity of these ecosystems in ways that are not yet fully understood (Seidl et al. 2017). Understanding both the nuances and potential of integrating the aforementioned measurements will create a more complete picture of the ENF carbon cycle. This is critical as both climate change and land-use decisions make the future of forests largely uncertain (Anderegg et al. 2020, Brodrigg et al. 2020). Long-term carbon storage and biodiversity of ENFs are hindered by interannual changes in temperature and precipitation as well as disturbance events linked to extreme weather, biotic agents, and large-scale demographic

shifts (Allen et al. 2010, Seidl et al. 2017, Anderegg et al. 2020). Both modeling and monitoring these changes have been challenging, with a recent study suggesting wide divergence in projections of future global forest vulnerability using the best available data and mechanistic models (Anderegg et al. 2022). Understanding how climate-sensitive disturbances might affect ENF vegetation physiology going forward will require multidisciplinary efforts for scaling and interpreting observations from the leaf to the globe.

We can glean essential knowledge of the environmental and physiological controls on the seasonality of ENF photosynthesis by combining fundamental theory of plant physiological ecology with a diverse combination of observations at scales from conifer needle to flux tower to satellite. In this Overview, we have shown how pigment-based thermal energy dissipation of excess sunlight is an integrative general property of ENFs response to adverse environmental conditions over both mild and harsh winters. In addition, we show that the steady-state emission of chlorophyll fluorescence can be a physiological indicator of ENF photosynthesis. Interpreting these processes from satellite data alone leaves out important nuances in these signals because of the low spatiotemporal resolution of satellite measurements. Therefore, without careful measurements of and expertise in plant pigments, gas exchange, and chlorophyll fluorescence at the site level interpretations of satellite products might over- or underestimate ENF photosynthetic seasonality. Colocated measurements of footprint-tower spectroscopy and needle biochemistry can provide an explanation for how seasonal adjustments in needle pigments and light energy partitioning are mechanistically linked to photosynthetic capacity. These crucial ground observations enable developers of satellite data products to correct for impacts of sun-sensor geometry and background noise that might

confound researchers' interpretation of SIF or pigment-based signals.

Although eddy covariance currently provides the best ground validation of remote-sensing derived ENF GPP products, both flux measurements and remote-sensing products carry uncertainties (Hollinger and Richardson 2005, Tramontana et al. 2015). Because flux measurements represent net exchanges of carbon, water, and energy at the ecosystem scale, flux data alone do not explicitly tell us the spatiotemporal contributions to or the partitioning of fluxes between different ecosystem components (Baldocchi 2003). Linking remote sensing with needle-scale measurements can help scientists interpret site-specific flux measurements by providing contextual information on community composition and vegetation function and help scale estimate fluxes globally (Ustin et al. 2009). Taken together, seasonal measurements of plant biochemistry or physiology, eddy covariance, and remote sensing can help paint a more complete picture of where uncertainties arise and how we might account for them going forward.

In this Overview, we show how coordinated measurement campaigns (figure 1) allow for a better understanding of the environmental controls on ENF physiology and, ultimately, how this can be approximated at multiple scales using remote-sensing products. With the rapid proliferation of new satellites and researchers using these data to draw conclusions about ecosystem response to climate change, the need remains for multidisciplinary efforts to better reconcile when, where, and to what extent remote sensing can be used to track changes in the carbon cycle. The multidisciplinary efforts discussed above involved experts in plant ecophysiology, leaf- and tower-scale carbon flux observations, and tower and satellite remote sensing. Going forward, empirical data from these efforts should be used to help inform modeling efforts or used in model-data fusion frameworks, requiring close collaboration with the ecosystem modeling community (Stofferahn et al. 2019, Gettelman et al. 2022). Accurate scaling of carbon cycle parameters from the site to the ecosystem to the biome is a major challenge but can be accomplished by well instrumented and monitored sites that encompass a broad range of ENFs. Doing so will ultimately enable scientists to better understand both the biological and physical drivers of changes in ENF photosynthesis and how we can accurately monitor and measure these processes under future climate scenarios.

Acknowledgments

This work was supported by National Science Foundation Macrosystems Biology and NEON-Enabled Science award no. 1926090 and National Science Foundation Division of Environmental Biology award no. 1929709. PhenoCam efforts have been supported by the National Science Foundation under grant no. EF-1702697. We were also supported by a National Science Foundation Graduate Research Fellowship under grants no. DGE-1650604 and no. DGE2034835, National Aeronautics and Space Administration ABoVE programs awards no. 80NSSC19M0130 and no. 80NSSC19M0129, NASA's Earth Science Division IDS awards no. 80NSSC17K0108 772 at UCLA and no. 80NSSC17K0110 at JPL, and National Aeronautics and Space Administration OCO Science team projects award no. 80NSSC18K0895. AJM and ZAP were partially supported by an appointment to the NASA Postdoctoral Program at the Jet Propulsion Laboratory, administered by Oak Ridge Associated Universities under contract with NASA. A portion of this research was carried out at the Jet Propulsion Laboratory, at the California Institute of Technology, under a contract with the National Aeronautics and Space Administration. The National

Ecological Observatory Network is a major facility fully funded by the National Science Foundation. Any opinion, findings, conclusions, or recommendations expressed in this material are those of the authors and do not necessarily reflect the views of the National Science Foundation.

Data and materials availability

Data for this publication are available at DOI:10.5281/zenodo.10048770.

Author contributions

Zoe Amie Pierrat (Conceptualization, Data curation, Formal analysis, Funding acquisition, Investigation, Methodology, Project administration, Supervision, Visualization, Writing – original draft, Writing – review & editing), Troy S. Magney (Conceptualization, Data curation, Formal analysis, Funding acquisition, Investigation, Methodology, Project administration, Resources, Supervision, Writing – original draft, Writing – review & editing), Rui Cheng (Data curation, Formal analysis, Writing – review & editing), Andrew J. Maguire (Data curation, Funding acquisition, Writing – review & editing), Christopher Y.S. Wong (Formal analysis, Visualization, Writing – original draft, Writing – review & editing), Magali F. Nehemy (Visualization, Writing – original draft, Writing – review & editing), Mukund Rao (Funding acquisition, Writing – original draft, Writing – review & editing), Sara E. Nelson (Data curation, Writing – original draft, Writing – review & editing), Anneka F. Williams (Data curation, Writing – original draft), Jeremy A. Hoyne Grosvenor (Data curation), Kenneth R. Smith (Data curation), Jaret S. Reblin (Conceptualization, Data curation, Writing – review & editing), Jochen Stutz (Supervision, Writing – review & editing), Andrew D. Richardson (Conceptualization, Data curation, Funding acquisition, Visualization, Writing – review & editing), Barry A. Logan (Conceptualization, Data curation, Funding acquisition, Methodology, Project administration, Resources, Supervision, Visualization, Writing – original draft, Writing – review & editing), and David R. Bowling (Conceptualization, Data curation, Formal analysis, Funding acquisition, Methodology, Project administration, Resources, Software, Supervision, Visualization, Writing – original draft, Writing – review & editing)

References cited

- Adams WW, Zarter CR, Ebbert V, Demmig-Adams B. 2004. Photoprotective strategies of overwintering evergreens. *BioScience* 54: 41–49.
- Alcaraz-Segura D, Chuvieco E, Epstein HE, Kasischke ES, Trishchenko A. 2010. Debating the greening vs. browning of the North American boreal forest: Differences between satellite datasets. *Global Change Biology* 16: 760–770.
- Allen CD, et al. 2010. A global overview of drought and heat-induced tree mortality reveals emerging climate change risks for forests. *Forest Ecology and Management* 259: 660–684.
- Anderegg WRL, Flint A, Huang C, Flint L, Berry JA, Davis FW, Sperry JS, Field CB. 2015. Tree mortality predicted from drought-induced vascular damage. *Nature Geoscience* 8: 367–371.
- Anderegg WRL, et al. 2020. Climate-driven risks to the climate mitigation potential of forests. *Science* 368: eaaz7005.
- Anderegg WRL, Chegwidden OS, Badgley G, Trugman A, Cullenward D, Abatzoglou JT, Hicke J, Freeman J, Hamman JJ. 2022. Future climate risks from stress, insects and fire across US forests. *Ecology Letters* 25: 1510–1520.

- Asner GP. 1998. Biophysical and biochemical sources of variability in canopy reflectance. *Remote Sensing of Environment* 64: 234–253.
- Atherton J, Olascoaga B, Alonso L, Porcar-Castell A. 2017. Spatial variation of leaf optical properties in a boreal forest is influenced by species and light environment. *Frontiers in Plant Science* 8: 309.
- Badgley G, Field CB, Berry JA. 2017. Canopy near-infrared reflectance and terrestrial photosynthesis. *Science Advances* 3: e1602244.
- Badgley G, Anderegg LDL, Berry JA, Field CB. 2019. Terrestrial gross primary production: Using NIRv to scale from site to globe. *Global Change Biology* 25: 3731–3740.
- Bai J, Zhang H, Sun R, Li X, Xiao J, Wang Y. 2022. Estimation of global GPP from GOME-2 and OCO-2 SIF by considering the dynamic variations of GPP-SIF relationship. *Agricultural and Forest Meteorology* 326: 109180.
- Baldocchi DD. 2003. Assessing the eddy covariance technique for evaluating carbon dioxide exchange rates of ecosystems: Past, present and future. *Global Change Biology* 9: 479–492.
- Baldocchi DD. 2020. How eddy covariance flux measurements have contributed to our understanding of global change biology. *Global Change Biology* 26: 242–260.
- Baldridge AM, Hook SJ, Grove CI, Rivera G. 2009. The ASTER spectral library version 2.0. *Remote Sensing of Environment* 113: 711–715.
- Beck PSA, Goetz SJ, Mack MC, Alexander HD, Jin Y, Randerson JT, Lorant MM. 2011. The impacts and implications of an intensifying fire regime on Alaskan boreal forest composition and albedo. *Global Change Biology* 17: 2853–2866.
- Beer C, et al. 2010. Terrestrial gross carbon dioxide uptake: Global distribution and covariation with climate. *Science* 329: 834–838.
- Bentz BJ, Jönsson AM, Schroeder M, Weed A, Wilcke RAI, Larsson K. 2019. *Ips typographus* and *Dendroctonus ponderosae* models project thermal suitability for intra- and inter-continental establishment in a changing climate. *Frontiers in Forests and Global Change* 2: 1.
- Berner LT, et al. 2020. Summer warming explains widespread but not uniform greening in the Arctic tundra biome. *Nature Communications* 11: 4621.
- Berry J, Bjorkman O. 1980. Photosynthetic response and adaptation to temperature in higher plants. *Annual Review of Plant Physiology* 31: 491–543.
- Bowling DR, Logan BA, Hufkens K, Aubrecht DM, Richardson AD, Burns SP, Anderegg WRL, Blanken PD, Eiriksson DP. 2018. Limitations to winter and spring photosynthesis of a Rocky Mountain subalpine forest. *Agricultural and Forest Meteorology* 252: 241–255.
- Brodribb TJ, Powers J, Cochard H, Choat B. 2020. Hanging by a thread? Forests and drought. *Science* 368: 261–266.
- Buermann W, et al. 2018. Widespread seasonal compensation effects of spring warming on northern plant productivity. *Nature* 562: 110.
- Butterfield Z, Buermann W, Keppel-Aleks G. 2020. Satellite observations reveal seasonal redistribution of northern ecosystem productivity in response to interannual climate variability. *Remote Sensing of Environment* 242: 111755.
- Chang CY, Zhou R, Kira O, Marri S, Skovira J, Gu L, Sun Y. 2020. An unmanned aerial system (UAS) for concurrent measurements of solar-induced chlorophyll fluorescence and hyperspectral reflectance toward improving crop monitoring. *Agricultural and Forest Meteorology* 294: 108145.
- Chen JM. 1996. Optically-based methods for measuring seasonal variation of leaf area index in boreal conifer stands. *Agricultural and Forest Meteorology* 80: 135–163.
- Cheng R, et al. 2020. Decomposing reflectance spectra to track gross primary production in a subalpine evergreen forest. *Biogeosciences* 17: 4523–4544.
- Cheng R, et al. 2022. Evaluating photosynthetic activity across arctic-boreal land cover types using solar-induced fluorescence. *Environmental Research Letters* 17: 115009.
- Comar CL, Zscheile FP. 1942. Analysis of plant extracts for chlorophylls a and b by a photoelectric spectrophotometric method. *Plant Physiology* 17: 198–209.
- Demmig-Adams B, Adams WW. 1992. Photoprotection and other responses of plants to high light stress. *Annual Review of Plant Physiology and Plant Molecular Biology* 43: 599–626.
- Demmig-Adams B, Adams WW. 2006. Photoprotection in an ecological context: The remarkable complexity of thermal energy dissipation. *New Phytologist* 172: 11–21.
- Desai AR, et al. 2008. Cross-site evaluation of eddy covariance GPP and RE decomposition techniques. *Agricultural and Forest Meteorology* 148: 821–838. doi:10.1016/j.agrformet.2007.11.012
- Dong J, Kaufmann RK, Myneni RB, Tucker CJ, Kauppi PE, Liski J, Buermann W, Alexeyev V, Hughes MK. 2003. Remote sensing estimates of boreal and temperate forest woody biomass: Carbon pools, sources, and sinks. *Remote Sensing of Environment* 84: 393–410.
- Doughty R, Köhler P, Frankenberg C, Magney TS, Xiao X, Qin Y, Wu X, Moore B. 2019. TROPOMI reveals dry-season increase of solar-induced chlorophyll fluorescence in the Amazon forest. *Proceedings of the National Academy of Sciences* 116: 22393–22398.
- Eitel JUH, Gessler PE, Smith AMS, Robberecht R. 2006. Suitability of existing and novel spectral indices to remotely detect water stress in *Populus* spp. *Forest Ecology and Management* 229: 170–182.
- Eklundh L, Johansson T, Solberg S. 2009. Mapping insect defoliation in Scots pine with MODIS time-series data. *Remote Sensing of Environment* 113: 1566–1573.
- Farquhar GD, von Caemmerer S, Berry JA. 1980. A biochemical model of photosynthetic CO₂ assimilation in leaves of C₃ species. *Planta* 149: 78–90.
- Felipe-Lucia MR, et al. 2018. Multiple forest attributes underpin the supply of multiple ecosystem services. *Nature Communications* 9: 4839.
- Fisher JB, et al. 2018. Missing pieces to modeling the arctic-boreal puzzle. *Environmental Research Letters* 13: 020202.
- Frankenberg C, Berry J. 2018. Solar induced chlorophyll fluorescence: Origins, relation to photosynthesis, and retrieval. Pages 143–162 in Liang S, ed. *Comprehensive Remote Sensing*. Elsevier.
- Frankenberg C, Butz A, Toon GC. 2011. Disentangling chlorophyll fluorescence from atmospheric scattering effects in O₂ A-band spectra of reflected sun-light. *Geophysical Research Letters* 38: L03801.
- Frankenberg C, O'Dell C, Berry J, Guanter L, Joiner J, Köhler P, Pollock R, Taylor TE. 2014. Prospects for chlorophyll fluorescence remote sensing from the Orbiting Carbon Observatory-2. *Remote Sensing of Environment* 147: 1–12.
- French NHF, et al. 2008. Using Landsat data to assess fire and burn severity in the North American boreal forest region: An overview and summary of results. *International Journal of Wildland Fire* 17: 443–462.
- Friedl M, Sulla-Menashe D. 2019. MCD12Q1 MODIS/Terra+Aqua Land Cover Type Yearly L3 Global 500m SIN Grid V006. Level 1 and Atmospheric Archive and Distribution System, Distributed Active Archive Center.
- Friedlingstein P, Meinshausen M, Arora VK, Jones CD, Anav A, Liddicoat SK, Knutti R. 2014. Uncertainties in CMIP5 climate projections due to carbon cycle feedbacks. *Journal of Climate* 27: 511–526.
- Friedlingstein P, et al. 2022. Global carbon budget 2021. *Earth System Science Data* 14: 1917–2005.

- Gamon JA. 2015. Reviews and syntheses: Optical sampling of the flux tower footprint. *Biogeosciences* 12: 4509–4523.
- Gamon JA, Peñuelas J, Field CB. 1992. A narrow-waveband spectral index that tracks diurnal changes in photosynthetic efficiency. *Remote Sensing of Environment* 41: 35–44.
- Gamon JA, Serrano L, Surfus JS. 1997. The photochemical reflectance index: An optical indicator of photosynthetic radiation use efficiency across species, functional types, and nutrient levels. *Oecologia* 112: 492–501.
- Gamon JA, Huemmrich KF, Stone RS, Tweedie CE. 2013. Spatial and temporal variation in primary productivity (NDVI) of coastal Alaskan tundra: Decreased vegetation growth following earlier snowmelt. *Remote Sensing of Environment* 129: 144–153.
- Gamon JA, Kovalchuck O, Wong CYS, Harris A, Garrity SR. 2015. Monitoring seasonal and diurnal changes in photosynthetic pigments with automated PRI and NDVI sensors. *Biogeosciences* 12: 4149–4159.
- Gamon JA, Huemmrich KF, Wong CYS, Ensminger I, Garrity S, Hollinger DY, Noormets A, Peñuelas J. 2016. A remotely sensed pigment index reveals photosynthetic phenology in evergreen conifers. *Proceedings of the National Academy of Sciences* 113: 13087–13092.
- Gao F, Masek J, Schwaller M, Hall F. 2006. On the blending of the Landsat and MODIS surface reflectance: Predicting daily Landsat surface reflectance. *IEEE Transactions on Geoscience and Remote Sensing* 44: 2207–2218.
- Garbulsky MF, Peñuelas J, Papale D, Ardö J, Goulden ML, Kiely G, Richardson AD, Rotenberg E, Veenendaal EM, Filella I. 2010. Patterns and controls of the variability of radiation use efficiency and primary productivity across terrestrial ecosystems. *Global Ecology and Biogeography* 19: 253–267.
- Gottelman A, Geer AJ, Forbes RM, Carmichael GR, Feingold G, Posselt DJ, Stephens GL, van den Heever SC, Varble AC, Zuidema P. 2022. The future of Earth system prediction: Advances in model-data fusion. *Science Advances* 8: eabn3488.
- Givnish TJ. 2002. Adaptive significance of evergreen vs. deciduous leaves: Solving the triple paradox. *Silva Fennica* 36: 535.
- Gonsamo A, Chen JM, Wu C, Dragoni D. 2012. Predicting deciduous forest carbon uptake phenology by upscaling FLUXNET measurements using remote sensing data. *Agricultural and Forest Meteorology* 165: 127–135.
- Grossmann K, Frankenberg C, Magney TS, Hurlock SC, Seibt U, Stutz J. 2018. PhotoSpec: A new instrument to measure spatially distributed red and far-red solar-induced chlorophyll fluorescence. *Remote Sensing of Environment* 216: 311–327.
- Guanter L, et al. 2021. The TROPISIF global sun-induced fluorescence dataset from the Sentinel-5P TROPOMI mission. *Earth System Science Data* 13: 5423–5440.
- He L, et al. 2020. From the ground to space: Using solar-induced chlorophyll fluorescence to estimate crop productivity. *Geophysical Research Letters* 47: e2020GL087474.
- Hikosaka K, Tsujimoto K. 2021. Linking remote sensing parameters to CO₂ assimilation rates at a leaf scale. *Journal of Plant Research* 134: 695–711.
- Hollinger DY, Richardson AD. 2005. Uncertainty in eddy covariance measurements and its application to physiological models. *Tree Physiology* 25: 873–885.
- Holt NE, Fleming GR, Niyogi KK. 2004. Toward an understanding of the mechanism of nonphotochemical quenching in green plants. *Biochemistry* 43: 8281–8289.
- Holzwarth AR, Jahns P. 2014. Non-photochemical quenching mechanisms in intact organisms as derived from ultrafast-fluorescence kinetic studies. Pages 129–156 in Demmig-Adams B, Garab G, Adams W III Govindjee, eds. *Non-Photochemical Quenching and Energy Dissipation in Plants, Algae and Cyanobacteria*. Springer Netherlands.
- Huner NPA, Öquist G, Hurry VM, Krol M, Falk S, Griffith M. 1993. Photosynthesis, photoinhibition and low temperature acclimation in cold tolerant plants. *Photosynthesis Research* 37: 19–39.
- Huxman TE, Turnipseed AA, Sparks JP, Harley PC, Monson RK. 2003. Temperature as a control over ecosystem CO₂ fluxes in a high-elevation, subalpine forest. *Oecologia* 134: 537–546.
- Jung M, et al. 2011. Global patterns of land-atmosphere fluxes of carbon dioxide, latent heat, and sensible heat derived from eddy covariance, satellite, and meteorological observations. *Journal of Geophysical Research: Biogeosciences* 116: G00J07.
- Jung M, et al. 2020. Scaling carbon fluxes from eddy covariance sites to globe: Synthesis and evaluation of the FLUXCOM approach. *Biogeosciences* 17: 1343–1365.
- Kautz M, Meddens AJH, Hall RJ, Arneth A. 2017. Biotic disturbances in Northern Hemisphere forests: A synthesis of recent data, uncertainties and implications for forest monitoring and modelling. *Global Ecology and Biogeography* 26: 533–552.
- Keenan TF, et al. 2014. Net carbon uptake has increased through warming-induced changes in temperate forest phenology. *Nature Climate Change* 4: 598–604.
- Keenan RJ, Reams GA, Achard F, de Freitas JV, Grainger A, Lindquist E. 2015. Dynamics of global forest area: Results from the FAO Global Forest Resources Assessment 2015. *Forest Ecology and Management* 352: 9–20.
- Köhl M, Lasco R, Cifuentes M, Jonsson Ö, Korhonen KT, Mundhenk P, de J, Stinson G. 2015. Changes in forest production, biomass and carbon: Results from the 2015 UN FAO Global Forest Resource Assessment. *Forest Ecology and Management* 352: 21–34.
- Kováč D, Ač A, Šigut L, Peñuelas J, Grace J, Urban O. 2022. Combining NDVI, PRI and the quantum yield of solar-induced fluorescence improves estimations of carbon fluxes in deciduous and evergreen forests. *Science of the Total Environment* 829: 154681.
- Lasslop G, Reichstein M, Papale D, Richardson AD, Arneth A, Barr A, Stoy P, Wohlfahrt G. 2010. Separation of net ecosystem exchange into assimilation and respiration using a light response curve approach: Critical issues and global evaluation. *Global Change Biology* 16: 187–208.
- Liu J, Wennberg PO, Parazoo NC, Yin Y, Frankenberg C. 2020a. Observational constraints on the response of high-latitude northern forests to warming. *AGU Advances* 1: e2020AV000228.
- Liu X, Liu L, Hu J, Guo J, Du S. 2020b. Improving the potential of red SIF for estimating GPP by downscaling from the canopy level to the photosystem level. *Agricultural and Forest Meteorology* 281: 107846.
- Logan BA. 2006. Oxygen metabolism and stress physiology. Pages 539–553 in Wise RR Hooper JK, eds. *The Structure and Function of Plastids*. Springer Netherlands.
- Logan BA, Grace SC, Iii WWA, Demmig-Adams B. 1998. Seasonal differences in xanthophyll cycle characteristics and antioxidants in *Mahonia repens* growing in different light environments. *Oecologia* 116: 9–17.
- Luus KA, et al. 2017. Tundra photosynthesis captured by satellite-observed solar-induced chlorophyll fluorescence. *Geophysical Research Letters* 44: 1564–1573.
- Luyssaert S, et al. 2007. CO₂ balance of boreal, temperate, and tropical forests derived from a global database. *Global Change Biology* 13: 2509–2537.
- Magney TS, et al. 2019. Mechanistic evidence for tracking the seasonality of photosynthesis with solar-induced fluorescence. *Proceedings of the National Academy of Sciences* 116: 11640–11645.

- Magney TS, Barnes ML, Yang X. 2020. On the covariation of chlorophyll fluorescence and photosynthesis across scales. *Geophysical Research Letters* 47: e2020GL091098.
- Maguire AJ, et al. 2020. On the functional relationship between fluorescence and photochemical yields in complex evergreen needle-leaf canopies. *Geophysical Research Letters* 47: e2020GL087858.
- Maguire AJ, Eitel JUH, Magney TS, Frankenberg C, Köhler P, Orcutt EL, Parazoo NC, Pavlick R, Pierrat ZA. 2021. Spatial covariation between solar-induced fluorescence and vegetation indices from arctic–boreal landscapes. *Environmental Research Letters* 16: 095002.
- Marrs JK, Reblin JS, Logan BA, Allen DW, Reinmann AB, Bombard DM, Tabachnik D, Hutyra LR. 2020. Solar-induced fluorescence does not track photosynthetic carbon assimilation following induced stomatal closure. *Geophysical Research Letters* 47: e2020GL087956.
- Maxwell K, Johnson GN. 2000. Chlorophyll fluorescence: A practical guide. *Journal of Experimental Botany* 51: 659–668.
- Meerdink SK, Hook SJ, Roberts DA, Abbott EA. 2019. The ECOSTRESS spectral library version 1.0. *Remote Sensing of Environment* 230: 111196.
- Michaelian M, Hogg EH, Hall RJ, Arsenault E. 2011. Massive mortality of aspen following severe drought along the southern edge of the Canadian boreal forest. *Global Change Biology* 17: 2084–2094.
- Mohammadi K, Jiang Y, Wang G. 2022. Flash drought early warning based on the trajectory of solar-induced chlorophyll fluorescence. *Proceedings of the National Academy of Sciences* 119: e2202767119.
- Mohammed GH, et al. 2019. Remote sensing of solar-induced chlorophyll fluorescence (SIF) in vegetation: 50 years of progress. *Remote Sensing of Environment* 231: 111177.
- Monteith JL. 1972. Solar radiation and productivity in tropical ecosystems. *Journal of Applied Ecology* 9: 747–766.
- Monteith JL. 1977. Climate and the efficiency of crop production in Britain. *Philosophical Transaction of the Royal Society B* 281: 277–294.
- Myers-Smith IH, et al. 2020. Complexity revealed in the greening of the Arctic. *Nature Climate Change* 10: 106–117.
- Myneni RB, Dong J, Tucker CJ, Kaufmann RK, Kauppi PE, Liski J, Zhou L, Alexeyev V, Hughes MK. 2001. A large carbon sink in the woody biomass of Northern forests. *Proceedings of the National Academy of Sciences* 98: 14784–14789.
- Nehemy MF, Maillet J, Perron N, Pappas C, Sonnentag O, Baltzer JL, Laroque CP, McDonnell JJ. 2022. Snowmelt water use at transpiration onset: Phenology, isotope tracing, and tree water transit time. *Water Resources Research* 58: e2022WR032344.
- Nehemy MF, Pierrat Z, Maillet J, Richardson AD, Stutz J, Johnson B, Helgason W, Barr AG, Laroque CP, McDonnell JJ. 2023. Phenological assessment of transpiration: The stem-temp approach for determining start and end of season. *Agricultural and Forest Meteorology* 331: 109319.
- Nelson PR, et al. 2022. Remote sensing of tundra ecosystems using high spectral resolution reflectance: Opportunities and challenges. *Journal of Geophysical Research: Biogeosciences* 127: e2021JG006697.
- Niyogi KK. 1999. Photoprotection revisited: Genetic and molecular approaches. *Annual Review of Plant Physiology and Plant Molecular Biology* 50: 333–359.
- Niyogi KK, Grossman AR, Björkman O. 1998. Arabidopsis mutants define a central role for the xanthophyll cycle in the regulation of photosynthetic energy conversion. *Plant Cell* 10: 1121–1134.
- Papale D, et al. 2006. Towards a standardized processing of net ecosystem exchange measured with eddy covariance technique: Algorithms and uncertainty estimation. *Biogeosciences* 3: 571–583.
- Pierrat Z, et al. 2021. Tower-based remote sensing reveals mechanisms behind a two-phased spring transition in a mixed-species boreal forest. *Journal of Geophysical Research: Biogeosciences* 126: e2020JG006191.
- Pierrat Z, et al. 2022a. Diurnal and seasonal dynamics of solar-induced chlorophyll fluorescence, vegetation indices, and gross primary productivity in the boreal forest. *Journal of Geophysical Research: Biogeosciences* 127: e2021JG006588.
- Pierrat ZA, Bortnik J, Johnson B, Barr A, Magney T, Bowling DR, Parazoo N, Frankenberg C, Seibt U, Stutz J. 2022b. Forests for forests: Combining vegetation indices with solar-induced chlorophyll fluorescence in random forest models improves gross primary productivity prediction in the boreal forest. *Environmental Research Letters* 17: 125006.
- Porcar-Castell A. 2011. A high-resolution portrait of the annual dynamics of photochemical and non-photochemical quenching in needles of *Pinus sylvestris*. *Physiologia Plantarum* 143: 139–153.
- Porcar-Castell A, Tyystjärvi E, Atherton J, van der Tol C, Flexas J, Pfundel EE, Moreno J, Frankenberg C, Berry JA. 2014. Linking chlorophyll a fluorescence to photosynthesis for remote sensing applications: Mechanisms and challenges. *Journal of Experimental Botany* 65: 4065–4095.
- Reichstein M, et al. 2005. On the separation of net ecosystem exchange into assimilation and ecosystem respiration: Review and improved algorithm. *Global Change Biology* 11: 1424–1439.
- Richardson AD. 2019. Tracking seasonal rhythms of plants in diverse ecosystems with digital camera imagery. *New Phytologist* 222: 1742–1750.
- Richardson AD, et al. 2018. Tracking vegetation phenology across diverse North American biomes using PhenoCam imagery. *Scientific Data* 5: 180028.
- Schimel D, Schneider FDJPL Carbon and Ecosystem participants. 2019. Flux towers in the sky: Global ecology from space. *New Phytologist* 224: 570–584.
- Schimel D, Pavlick R, Fisher JB, Asner GP, Saatchi S, Townsend P, Miller C, Frankenberg C, Hibbard K, Cox P. 2015. Observing terrestrial ecosystems and the carbon cycle from space. *Global Change Biology* 21: 1762–1776.
- Schreiber U. 2004. Pulse-amplitude-modulation (PAM) fluorometry and saturation pulse method: An overview. Pages 279–319 in Pappas C, Govindjee, eds. *Chlorophyll a Fluorescence: A Signature of Photosynthesis*. Springer Netherlands.
- Seidl R, et al. 2017. Forest disturbances under climate change. *Nature Climate Change* 7: 395–402.
- Serbin SP, Ahl DE, Gower ST. 2013. Spatial and temporal validation of the MODIS LAI and FPAR products across a boreal forest wildfire chronosequence. *Remote Sensing of Environment* 133: 71–84.
- Sevanto S, Suni T, Pumpanen J, GrÅnholm T, Kolari P, Nikinmaa E, Hari P, Vesala T. 2006. Wintertime photosynthesis and water uptake in a boreal forest. *Tree Physiology* 26: 749–757.
- Seyednasrollah B, et al. 2021. Seasonal variation in the canopy color of temperate evergreen conifer forests. *New Phytologist* 229: 2586–2600.
- Shen Q, Liu L, Zhao W, Yang J, Han X, Tian F, Wu J. 2021. Relationship of surface soil moisture with solar-induced chlorophyll fluorescence and normalized difference vegetation index in different phenological stages: A case study of Northeast China. *Environmental Research Letters* 16: 024039.
- Sims DA, Luo H, Hastings S, Oechel WC, Rahman AF, Gamon JA. 2006. Parallel adjustments in vegetation greenness and ecosystem CO₂ exchange in response to drought in a Southern California chaparral ecosystem. *Remote Sensing of Environment* 103: 289–303.

- Smith WB, Miles PD, Perry CH, Pugh SA. 2009. Forest Resources of the United States 2007: A Technical Document Supporting the Forest Service 2010 RPA Assessment. USDA Forest Service
- Smith WK, Fox AM, MacBean N, Moore DJP, Parazoo NC. 2020. Constraining estimates of terrestrial carbon uptake: New opportunities using long-term satellite observations and data assimilation. *New Phytologist* 225: 105–112.
- Sperry JS, Sullivan JEM. 1992. Xylem embolism in response to freeze-thaw cycles and water stress in ring-porous, diffuse-porous, and conifer species. *Plant Physiology* 100: 605–613.
- Steinberg DC, Goetz SJ, Hyer EJ. 2006. Validation of MODIS F/sub PAR/products in boreal forests of Alaska. *IEEE Transactions on Geoscience and Remote Sensing* 44: 1818–1828.
- Stofferahn E, Fisher JB, Hayes DJ, Schwalm CR, Huntzinger DN, Hantson W, Poulter B, Zhang Z. 2019. The arctic-boreal vulnerability experiment model benchmarking system. *Environmental Research Letters* 14: 055002.
- Sun Y, Frankenberg C, Jung M, Joiner J, Guanter L, Köhler P, Magney T. 2018. Overview of solar-induced chlorophyll fluorescence (SIF) from the Orbiting Carbon Observatory-2: Retrieval, cross-mission comparison, and global monitoring for GPP. *Remote Sensing of Environment* 209: 808–823.
- Tramontana G, Ichii K, Camps-Valls G, Tomelleri E, Papale D. 2015. Uncertainty analysis of gross primary production upscaling using random forests, remote sensing and eddy covariance data. *Remote Sensing of Environment* 168: 360–373.
- Tramontana G, Migliavacca M, Jung M, Reichstein M, Keenan TF, Camps-Valls G, Ogee J, Verrelst J, Papale D. 2020. Partitioning net carbon dioxide fluxes into photosynthesis and respiration using neural networks. *Global Change Biology* 26: 5235–5253.
- Trugman AT, Anderegg LDL, Anderegg WRL, Das AJ, Stephenson NL. 2021. Why is tree drought mortality so hard to predict? *Trends in Ecology and Evolution* 36: 520–532.
- Tucker CJ. 1979. Red and photographic infrared linear combinations for monitoring vegetation. *Remote Sensing of Environment* 8: 127–150.
- Ustin SL, Gitelson AA, Jacquemoud S, Schaepman M, Asner GP, Gamon JA, Zarco-Tejada P. 2009. Retrieval of foliar information about plant pigment systems from high resolution spectroscopy. *Remote Sensing of Environment* 113: S67–S77.
- van der Tol C, Berry JA, Campbell PKE, Rascher U. 2014. Models of fluorescence and photosynthesis for interpreting measurements of solar-induced chlorophyll fluorescence. *Journal of Geophysical Research: Biogeosciences* 119: 2014JG002713.
- Verhoeven A. 2014. Sustained energy dissipation in winter evergreens. *New Phytologist* 201: 57–65.
- Walther S, Voigt M, Thum T, Gonsamo A, Zhang Y, Köhler P, Jung M, Varlagin A, Guanter L. 2016. Satellite chlorophyll fluorescence measurements reveal large-scale decoupling of photosynthesis and greenness dynamics in boreal evergreen forests. *Global Change Biology* 22: 2979–2996.
- Wang JA, Friedl MA. 2019. The role of land cover change in arctic-boreal greening and browning trends. *Environmental Research Letters* 14: 125007.
- Wang X, Chen JM, Ju W. 2020. Photochemical reflectance index (PRI) can be used to improve the relationship between gross primary productivity (GPP) and sun-induced chlorophyll fluorescence (SIF). *Remote Sensing of Environment* 246: 111888.
- Wang R, et al. 2023. Snow-corrected vegetation indices for improved gross primary productivity assessment in North American evergreen forests. *Agricultural and Forest Meteorology* 340: 109600.
- White MA, et al. 2009. Intercomparison, interpretation, and assessment of spring phenology in North America estimated from remote sensing for 1982–2006. *Global Change Biology* 15: 2335–2359.
- Wong CYS, Gamon JA. 2015a. The photochemical reflectance index provides an optical indicator of spring photosynthetic activation in evergreen conifers. *New Phytologist* 206: 196–208.
- Wong CYS, Gamon JA. 2015b. Three causes of variation in the photochemical reflectance index (PRI) in evergreen conifers. *New Phytologist* 206: 187–195.
- Wong CYS, Mercado LM, Arain MA, Ensminger I. 2022. Remotely sensed carotenoid dynamics improve modelling photosynthetic phenology in conifer and deciduous forests. *Agricultural and Forest Meteorology* 321: 108977.
- Wutzler T, Lucas-Moffat A, Migliavacca M, Knauer J, Sickel K, Šigut L, Menzer O, Reichstein M. 2018. Basic and extensible post-processing of eddy covariance flux data with REddyProc. *Biogeosciences* 15: 5015–5030.
- Xiao J, et al. 2019. Remote sensing of the terrestrial carbon cycle: A review of advances over 50 years. *Remote Sensing of Environment* 233: 111383.
- Yang X, Tang J, Mustard JF, Lee JE, Rossini M, Joiner J, Munger JW, Kornfeld A, Richardson AD. 2015. Solar-induced chlorophyll fluorescence that correlates with canopy photosynthesis on diurnal and seasonal scales in a temperate deciduous forest. *Geophysical Research Letters* 42: 2977–2987.
- Yang JC, Magney TS, Yan D, Knowles JF, Smith WK, Scott RL, Barron-Gafford GA. 2020. The photochemical reflectance index (PRI) captures the ecohydrologic sensitivity of a semiarid mixed conifer forest. *Journal of Geophysical Research: Biogeosciences* 125: e2019JG005624.
- Yang JC, et al. 2022. Gross primary production (GPP) and red solar induced fluorescence (SIF) respond differently to light and seasonal environmental conditions in a subalpine conifer forest. *Agricultural and Forest Meteorology* 317: 108904.
- Zeng Y, Badgley G, Dechant B, Ryu Y, Chen M, Berry JA. 2019. A practical approach for estimating the escape ratio of near-infrared solar-induced chlorophyll fluorescence. *Remote Sensing of Environment* 232: 111209.
- Zeng Y, et al. 2022. Optical vegetation indices for monitoring terrestrial ecosystems globally. *Nature Reviews Earth and Environment* 3: 477–493.
- Zhang X, Friedl MA, Schaaf CB, Strahler AH, Hodges JCF, Gao F, Reed BC, Huete A. 2003. Monitoring vegetation phenology using MODIS. *Remote Sensing of Environment* 84: 471–475.